PROCESS DEVELOPMENT FOR THE SYNTHESES OF ESSENTIAL MEDICINES IN CONTINUOUS FLOW

by

Robert J. Nicholas

A Thesis

Submitted to the Faculty of Purdue University

In Partial Fulfillment of the Requirements for the degree of

Master of Science

Department of Chemistry

West Lafayette, Indiana

May 2022

THE PURDUE UNIVERSITY GRADUATE SCHOOL

STATEMENT OF COMMITTEE APPROVAL

Dr. David H. Thompson, Chair

Department of Chemistry

Dr. Bryan W. Boudouris

Department of Chemical Engineering

Dr. Mingji Dai

Department of Chemistry

Approved by:

Dr. Christine Hrycyna

In loving memory of Charles L. Henry: Grandfather, friend, and servant of Christ
(1927 - 2018)

ACKNOWLEDGMENTS

I would like to thank my advisor Dr. David Thompson for the privilege to work in his lab and for teaching me what it means to be an effective chemist. I will carry the skills I have learned with me for life. I know that I will effectively apply what I have learned in my future pursuits.

I want to also thank the current and previous members of the Thompson group for their comradery and support. I grew to consider them as a second family. I also want to thank Continuity Pharma LLC, specifically Dr. Michael McGuire and Dr. Seok-Hee Hyun, for their collaboration and for the experience working in a start-up culture.

I thank my parents, Bob and Sharon Nicholas, as well as my extended family for their continual love and support. I know that I have made them proud. I also want to thank my Lord and Savior Jesus Christ for the hope that he brings as I continue my daily walk to be more like him.

Finally, I want to thank the Purdue Department of Chemistry and the Purdue Cancer Research Center for helping fund this work.

TABLE OF CONTENTS

LIST OF TABLES

LIST OF FIGURES

ABSTRACT

A significant number of resources are allocated to maintaining the resiliency of pharmaceutical supply chain as failure to do so thoroughly can result in drug shortages of essential medicines. Recently, the effects of COVID-19 exacerbated flaws in the current system causing the pharmaceutical industry and government organizations and to reassess relief strategies that could also strengthen the supply chain. Flow chemistry has become an attractive and prominent platform enabling continuous manufacturing (CM) technologies to synthesize active pharmaceutical ingredients (API) quickly according to demand. Compared to traditional batch chemistry, flow chemistry has demonstrated to be more robust in terms of throughput, scalability, and hazard reduction while maintaining a high degree of control and product quality. This work demonstrates these capabilities in reaction optimization and discovery with the overarching goal of domesticating CM to make essential medicines more affordable. A two-step process for the synthesis in diazepam was developed using a Chemtrix Labtrix S1 and Start microfluidic systems where purities as high as 98% were achieved. The system was successfully scaled up to a larger system that was able to produce 96% pure diazepam at a 91% yield.

CHAPTER 1. INTRODUCTION

1.1 Pharmaceutical Supply Chains

Supply chains of essential goods are essential in maintaining national security and economy. These networks are comprised of various roles including suppliers, manufactures, and distributors that help bring a product to the consumer. Safeguards such as resource diversification and manufacturing redundancy are usually implemented to prevent disruptions that could otherwise compromise the integrity of a supply chain.[1] Nevertheless, external pressures like market demand put a strain on supply chains and can potentially cause a shortage of goods. This was especially the case during the COVID-19 pandemic as it exposed multiple shortcomings in the current infrastructure for supply chains in multiple markets including lumber[2] and computer chips.[3] The pharmaceutical market in particular saw heightened demand for multiple drugs.[4-6] This reinforced the need for the pharmaceutical industry to create robust and resilient supply chains to deliver quality medicines to patients should another crisis occur.

A typical pharmaceutical supply chain is depicted in Figure 1.1. Initially, suppliers will gather up raw materials from natural sources where they can be refined into fine chemicals such as solvents or reagents. These fine chemicals are sold to manufacturers to be employed at different steps of a drug synthesis. A manufacturer may choose to perform the entire synthesis in-house or synthesize a key intermediate of an active pharmaceutical ingredient (API) and have it shipped to another site; however, implementation of the latter will make the supply chain more complex as it adds additional steps in the chain. Once the final API is produced and up to purity standards, it is combined with other benign excipients (e.g. cellulose) into a usable drug product such as a tablet or injectable. This is the product that gets distributed into the market through healthcare facilities or other intermediaries for patient use.

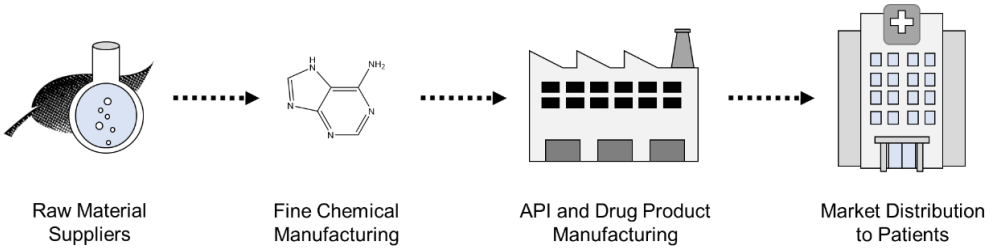

Figure 1.1 Schematic of a pharmaceutical supply chain. Raw materials are transformed into fine chemicals that are used to synthesize API. The final drug gets distributed to patients.

The susceptibility of pharmaceutical supply chains has been a rising concern in recent years as there is a growing dependency on international sources due to drug manufacturing jobs gradually moving outside of the U.S.[7] The U.S. Food and Drug Administration (FDA) reported that only 28% of global API manufacturing is done in the U.S. as of 2019.[8] Of the remaining 72%, China and India make up 13% and 18%, respectively, of API manufacturing and are projected to increase (Figure 1.2).[8] A main contributor as to why foreign countries like China and India are seeing growth in this field is because of low-cost labor and utilities as well as less stringent regulations. This incentivizes companies to construct new facilities in these countries thus adding complexity the drug supply chains and increasing the risk for drug shortages. During the COVID-19 pandemic, countries limited exports as they were concerned about providing medicines and other resources to their own citizens thus leading to global shortages of certain essential medicines.[5,9]

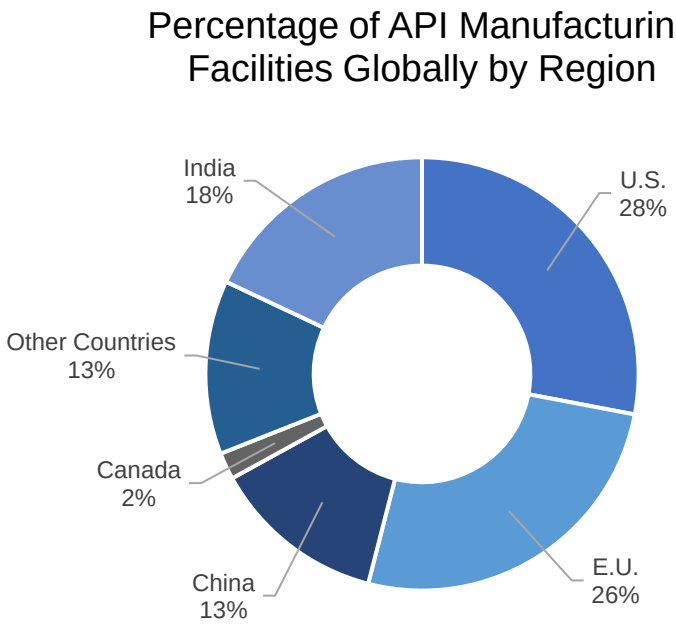

Figure 1.2 Percentage of API manufacturing facility globally by region.[8]

Drug shortages are a multifactorial issue that can result from complications aside from foreign outsourcing. For example, supply issues can arise whenever manufacturers are unable or unwilling to produce enough API to meet a demand. These may include manufacturing problems like poor quality production, raw materials becoming unavailable or too expensive, or logistical issues including the aforementioned international dependency.[10] Market demand can also contribute towards a drug shortage. Just-in-time inventory systems schedule production based on a calculated demand in order to maximize profits; however, unpredictable increases in demand may occur due to an epidemic or disaster thus throwing off projections and leading to a shortage.[6] This is especially detrimental if a buffer stock is not accounted for during production as manufacturers must quickly produce and distribute the medicines. Ultimately, a drug shortage can impair a patient's healthcare as they may be unable to receive proper treatment.

Taking these vulnerabilities into consideration, drug manufacturers may take preventative measures to avoid possible drug shortages. One tactic is to obtain raw materials from multiple suppliers instead of a single source.[11] They may also choose to be more proactive and transparent in communication with regulatory authorities like the FDA or company shareholders in order to make more proactive decisions should signs of a potential shortage arise.[12] During an ongoing shortage, a company may ramp up production to meet demand or reallocate their current stock to

assist areas in more dire need. The FDA may sanction Emergency Use Authorizations upon performing a risk assessment. This may include being more lenient on quality standards for medicines with minor defects or increasing the expiratory date of a drug lot. Examples of both of these latter instances occurred during the height of the COVID-19 pandemic.[13,14]

Another innovation that the industry is looking into is advanced manufacturing. This includes cutting-edge technologies that are able to enhance the quality and production of drugs or drug products making this a viable option for defense against shortages. Examples of these include continuous manufacturing (CM) and 3-D printing. Although there is a large upfront cost associated, these technologies may become advantageous in the long run as medicines can be produced at lower costs than by traditional means.[15] Quality can be more precisely controlled and in real-time given the automated nature of the systems and in-line process analytical technology. Scalability is also highly flexible which becomes important if production needs to accommodate accordingly to the unpredictable changes in demand. This, along with the fact that these systems often have a smaller footprint and environmental factor (E-factor), makes advanced manufacturing an attractive, economic option that the pharmaceutical industry is beginning to adopt. It is expected that this technology can restore competitiveness of domestic manufacturing and ensure a more stable supply of drugs for the U.S. market.[8] Ongoing research and development efforts into new applications of advanced manufacturing has ramifications to bolster the resiliency of pharmaceutical supply chains.

1.2 Continuous Flow Chemistry

An advanced manufacturing platform that has gained traction within industry and academia is CM via flow chemistry. When compared to batch chemistry, both methods are analogous in the sense that parameters such as reaction time and temperature can be manipulated; however, flow chemistry differs from traditional batch chemistries as chemical transformations occur as the materials travel through reactor channels as opposed to being stirred in a flask or vat. This unique platform offers its own unique advantages compared to batch such as improved mixing, control, safety, atom economy, and heat transfer (Figure 1.3).[16,17] These may optimize a reaction in flow by inducing a higher yield, enhancing volume-time output, reducing E-factor, and improving cost efficiency. Additionally, flow chemistry can be used to screen reactions and possibly achieve reactions that are otherwise difficult or not possible in batch.[18-21]

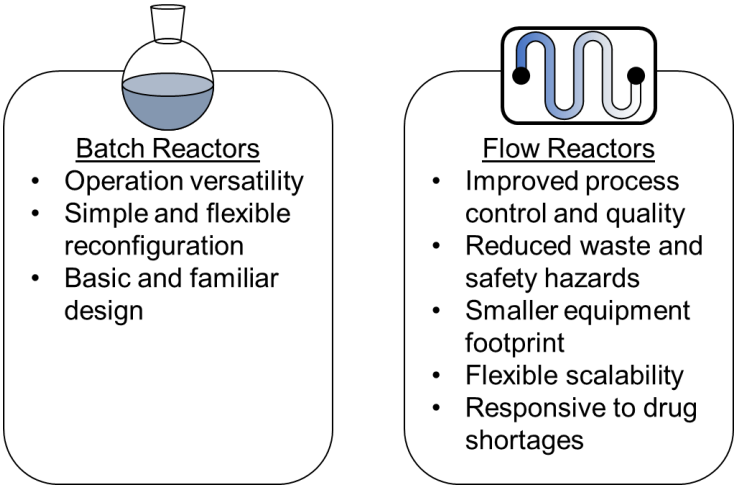

Figure 1.3 Comparison of benefits between batch and flow reactors.

While flow may have advantages over batch, it should be noted that flow is not always the preferred method. For example, systems that require a stoichiometric amount of a solid reagent would be more suitable in a batch reactor as the solid may clog the flow reactor channels. In a similar vein, reactions that generate a precipitate also have a propensity of fouling a flow reactor. Heterogeneous systems can be achieved in flow via installation of a packed bed reactor. These will typically contain a solid catalyst or resin to drive a reaction forward or to clean up any impurities. The solids may need to be exchanged with new unreacted solid or have to undergo a reactivation process to maintain reactivity. A batch set-up is also a familiar design, and some may prefer its simplicity over flow.

The pharmaceutical industry is starting to see a shift towards CM. Vertex became a pioneer with their cystic fibrosis treatment Orkambi as it was the first drug to have a CM process approved by the FDA in 2015.[22] The following year, Janssen switched production of Prezista, an HIV antiviral, from batch manufacturing to CM where it was also approved by the FDA.[22] Currently, the FDA has approved 6 drugs that are produced using CM with more anticipated to come (Table 1.1). Drugs like remdesivir have been investigated in flow chemistry to mitigate risks associated with hazardous reagents while maintaining tight control of reaction parameters at a large scale.[23] In the academic sphere, an MIT group designed a reconfigurable CM platform to synthesize 5 essential generic APIs as part of an effort towards the Pharmacy on Demand initiative.[24] These endeavors support the growing trend of CM and may lead to more resistant pharmaceutical supply

chains whether it encourages companies to produce drugs domestically or have effective platforms to meet demand rapidly and accurately.

Table 1.1 List of drugs currently approved by the FDA for CM.[17]

Product	Company	Approval Date	Treatment
Orkambi (Lumacaftor/Ivacaftor)	Vertex Pharmaceuticals	July 2015	Cystic fibrosis
Prezista (Darunavir)	Janssen Pharmaceuticals	April 2016	HIV
Verzenio (Abemaciclib)	Eli Lilly & Co.	September 2017	Breast Cancer
Symdeko/Symkevi (Tezacaftor/Ivacaftor)	Vertex Pharmaceuticals	February 2018	Cystic fibrosis
Daurismo (Glasdegib)	Pfizer Inc.	November 2018	Acute myeloid leukemia (AML)
Trikafta (Elexacaftor/ Tezacaftor/Ivacaftor)	Vertex Pharmaceuticals	October 2019	Cystic fibrosis

Flow reactions conducted as a part of this work were achieved mainly using a Chemtrix Labtrix S1 reactor (Figure 1.4). This system is fitted with five syringe pumps whose flow rates can be controlled through a computer with proprietary software. The syringes can dispense solutions through a glass microreactor chip that is positioned on a Peltier block where the temperature can also be controlled by software. The final solution is dispensed through a stainless-steel needle. The flow system can also be fitted with a back pressure regulator (BPR) so that reactions requiring higher pressures can be achieved. This is especially useful for volatile solvents or reagents.

The main utility of this system lies in its ability to screen multiple reaction conditions in one automated experiment making it ideal for Design of Experiments (DoE). For example, variables such as temperature, residence time, stoichiometry, and flow rate of a specific reaction can be quickly evaluated by testing two or more variables at a time thus rapidly optimizing for highest yield or cleanest impurity profile. The installed carousel can hold up to 30 HPLC vials at a time which can be used to collect fractions of a reaction at different timepoints or conditions which can be analyzed with instrumentation such as LC-MS.

Microfluidic experiments were not just limited to the S1 system as we were able to telescope two reactions using a Labtrix Start reactor. While the Start system is primarily just a chip

holder with a Peltier block, reagents mounted on the S1 system can be directed into the reactor chip situated in the Start system where it can flow into the second reactor in the S1 system. It is also possible to use off-line syringe pumps; however, the ability to automate the flowrates of those pumps is lost as they are not connected to the Chemtrix software.

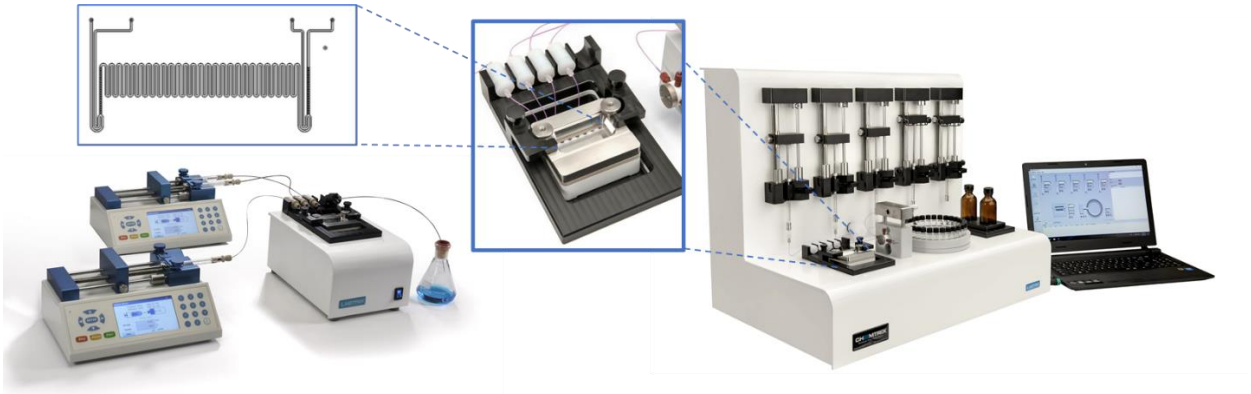

Figure 1.4. Depiction of Chemtrix Labtrix Start and S1 microfluidic reactors. Labtrix Start (bottom left) and S1 (right) systems were used for reaction discovery and optimization. Reactor holder (middle) and microreactor chip (top left) are also visualized. Images were gathered from Chemtrix company website.

1.3 References

[1] Hendricks, K. B.; Singhal, V. R.; Zhang, R. The Effect of Operational Slack, Diversification, and Vertical Relatedness on the Stock Market Reaction to Supply Chain Disruptions. *J. Oper. Manag.* **2009**, *27*, 233-246.

[2] van Kooten, G. C.; Schmitz, A. COVID-19 Impacts on U.S. Lumber Markets. *For. Policy Econ.* **2022**, *135*, 102665.

[3] Akcil, A.; Sun, Z.; Panda, S. COVID-19 Disruptions to Tech-Metals Supply Are a Wake-up Call. *Nature* **2020**, *587*, 365–367.

[4] Ammar, M. A.; Sacha, G. L.; Welch, S. C.; Bass, S. N.; Kane-Gill, S. L.; et al. Sedation, Analgesia, and Paralysis in COVID-19 Patients in the Setting of Drug Shortages. *J. Intensive Care Med.* **2021**, *36*, 157–174.

[5] Ayati, N.; Saiyarsarai, P.; Nikfar, S. Short and Long Term Impacts of COVID-19 on the Pharmaceutical Sector. *DARU J. Pharm. Sci.* **2020**, *28*, 799–805.

[6] Shukar, S.; Zahoor, F.; Hayat, K.; Saeed, A.; Gillani, A. H.; et al. Drug Shortage: Causes, Impact, and Mitigation Strategies. *Front. Pharmacol.* **2021**, *12*, 693426.

[7] Fort, T. C.; Pierce, J. R.; Schott, P. K. New Perspectives on the Decline of US anufacturing Employment. *J. Econ. Perspect.* **2018**, *32*, 47–72.

[8] Woodcock, J. Safeguarding Pharmaceutical Supply Chains in a Global Economy, 2019. U.S. Food and Drug Administration Web site. https://www.fda.gov/news-events/congressional-testimony/safeguarding-pharmaceutical-supply-chains-global-economy-10302019 (accessed Mar 10, 2022).

[9] Barlow, P.; Schalkwyk, M. C. van; McKee, M.; Labonté, R.; Stuckler, D. COVID-19 and the Collapse of Global Trade: Building an Effective Public Health Response. *Lancet Planet. Health* **2021**, *5*, e102–e107.

[10] Dill, S.; Ahn, J. Drug Shortages in Developed Countries—Reasons, Therapeutic Consequences, and Handling. *Eur. J. Clin. Pharmacol.* **2014**, *70*, 1405–1412.

[11] Hedman, L. Global Approaches to Addressing Shortages of Essential Medicines in Health Systems. *WHO Drug Inf.* **2016**, *30*, 180–185.

[12] Costelloe, E. M.; Guinane, M.; Nugent, F.; Halley, O.; Parsons, C. An Audit of Drug Shortages in a Community Pharmacy Practice. *Ir. J. Med. Sci.* **2015**, 184, 435–440.

[13] Tran, A.; Witek, T. J. The Emergency Use Authorization of Pharmaceuticals: History and Utility During the COVID-19 Pandemic. *Pharm. Med*. **2021**, *35*, 203–213.

[14] Zuckerman, D. M. Emergency Use Authorizations (EUAs) Versus FDA Approval: Implications for COVID-19 and Public Health. *Am. J. Public Health* **2021**, *111*, 1065–1069.

[15] Helal, N. A.; Elnoweam, O.; Eassa, H. A.; Amer, A. M.; Eltokhy, M. A.; et al. Integrated Continuous Manufacturing in Pharmaceutical Industry: Current Evolutionary Steps toward Revolutionary Future. *Pharm. Pat. Anal*. **2019**, *8*, 139–161.

[16] McQuade, D. T.; Seeberger, P. H. Applying Flow Chemistry: Methods, Materials, and Multistep Synthesis. *J. Org. Chem*. **2013**, *78*, 6384–6389.

[17] Hock, S. C.; Siang, T. K.; Wah, C. L. Continuous Manufacturing Versus Batch Manufacturing: Benefits, Opportunities and Challenges for Manufacturers and Regulators. *GaBI Journal* **2021**, *10*, 44-56.

[18] Malet-Sanz, L.; Susanne, F. Continuous Flow Synthesis. A Pharma Perspective. *J. Med. Chem*. **2012**, *55*, 4062–4098.

[19] Bédard, A.-C.; Adamo, A.; Aroh, K. C.; Russell, M. G.; Bedermann, A. A.; et al. Reconfigurable System for Automated Optimization of Diverse Chemical Reactions. *Science* **2018**, *361*, 1220–1225.

[20] Jaman, Z.; Logsdon, D. L.; Szilágyi, B.; Sobreira, T. J. P.; Aremu, D.; et al. High-Throughput Experimentation and Continuous Flow Evaluation of Nucleophilic Aromatic Substitution Reactions. *ACS Comb. Sci*. **2020**, *22*, 184–196.

[21] Loren, B. P.; Wleklinski, M.; Koswara, A.; Yammine, K.; Hu, Y.; et al. Mass Spectrometric Directed System for the Continuous-Flow Synthesis and Purification of Diphenhydramine. *Chem. Sci*. **2017**, *8*, 4363–4370.

[22] Vanhoorne, V.; Vervaet, C. Recent Progress in Continuous Manufacturing of Oral Solid Dosage Forms. *Int. J. Pharm*. **2020**, *579*, 119194.

[23] Vieira, T.; Stevens, A. C.; Chtchemelinine, A.; Gao, D.; Badalov, P.; Heumann, L. Development of a Large-Scale Cyanation Process Using Continuous Flow Chemistry En Route to the Synthesis of Remdesivir. *Org. Process Res. Dev*. **2020**, *24*, 2113–2121.

[24] Rogers, L.; Briggs, N.; Achermann, R.; Adamo, A.; Azad, M.; et al. Continuous Production of Five Active Pharmaceutical Ingredients in Flexible Plug-and-Play Modules: A Demonstration Campaign. *Org. Process Res. Dev*. **2020**, *24*, 2183–2196.

CHAPTER 2. DEVELOPMENT OF AN EFFICIENT HIGH PURITY CONTINUOUS FLOW SYNTHESIS OF DIAZEPAM

This chapter was originally submitted for publication in *Frontiers in Chemical Engineering*: Nicholas, R.J.; McGuire, M.A.; Hyun, S.-H.; Cullison, M.N.; Thompson D.H., *Front. Chem. Eng.*, **2022**, in review.

2.1 Introduction

The stability and reliability of drug supply chains are crucial for maintaining quality patient care. Unfortunately, there are multiple factors that contribute to supply chain fragility and rapid changes in market demand, leaving manufacturers unable to adequately respond with their current infrastructure and production processes.[1] This liability is further compounded by the just-in-time inventory systems that are practiced by multiple pharmaceutical companies in order to keep waste and inventory costs low.[2] The U.S. Food and Drug Administration (FDA) has been encouraging the pharmaceutical industry to pursue continuous manufacturing (CM) to address the supply chain issue by providing greater responsiveness, robustness, and higher product quality as opposed to batch processes.[3] In a striking example of the responsiveness possible, CM enabled the controlled encapsulation of mRNA in lipid nanoparticles at unprecedented speeds to successfully distribute millions of COVID-19 vaccines globally at the height of the pandemic.[4]

Continuous flow synthesis of various active pharmaceutical ingredients (APIs) by academic and industrial groups has been well documented.[5-9] One API of interest is diazepam, a fast-acting anxiolytic, that is considered an essential medicine by the World Health Organization[10] and is among the top 200 drugs prescribed in the U.S.[11] Unfortunately, diazepam is a drug that is very susceptible to shortages and may contribute to price and/or demand increase of other benzodiazepines when in short supply.[12] Developing a robust, scalable CM process for diazepam is timely given the upward trends in prescription rates[13,14] making it a worthy target for process optimization.

Various publications document the continuous synthesis of diazepam in two key steps: *N*-acylation and sequential substitution/cyclization reactions, starting from 5-chloro-2-(methylamino)benzophenone (**1**) (Figure 2.1a and 2.1b). Previously, our group used high throughput experimentation to identify conditions for the synthesis of diazepam.[15] Using a toluene

and methanol solvent system, they were able to achieve 70% pure diazepam using a microfluidic reactor. Adamo *et al.* engineered a process as part of their reconfigurable manufacturing platform where they dissolved their reagents in NMP to produce 78% of crude target API according to HPLC analysis.[16] The collected API was obtained in 94% yield. This same process was implemented in a subsequent publication by Rogers *et al.* describing the production of 2800 dose equivalents that met USP standards.[17] Collins *et al.* developed an automated platform called AutoSyn to synthesize API.[18] For their two-step synthesis of diazepam, they collected a 96% yield with 81% pure API with the other 19% being reaction intermediate **3b**. Bédard *et al.* focused on eliminating waste in their flow process to improve the E-factor.[19] While they were only able to obtain a 55% yield, they reduced the E-factor of the method first reported by Adamo *et al.* from 36 to 9, primarily by using 2-MeTHF, a solvent immiscible with water, instead of NMP to enable in-line aqueous extractions without needing extra solvent.

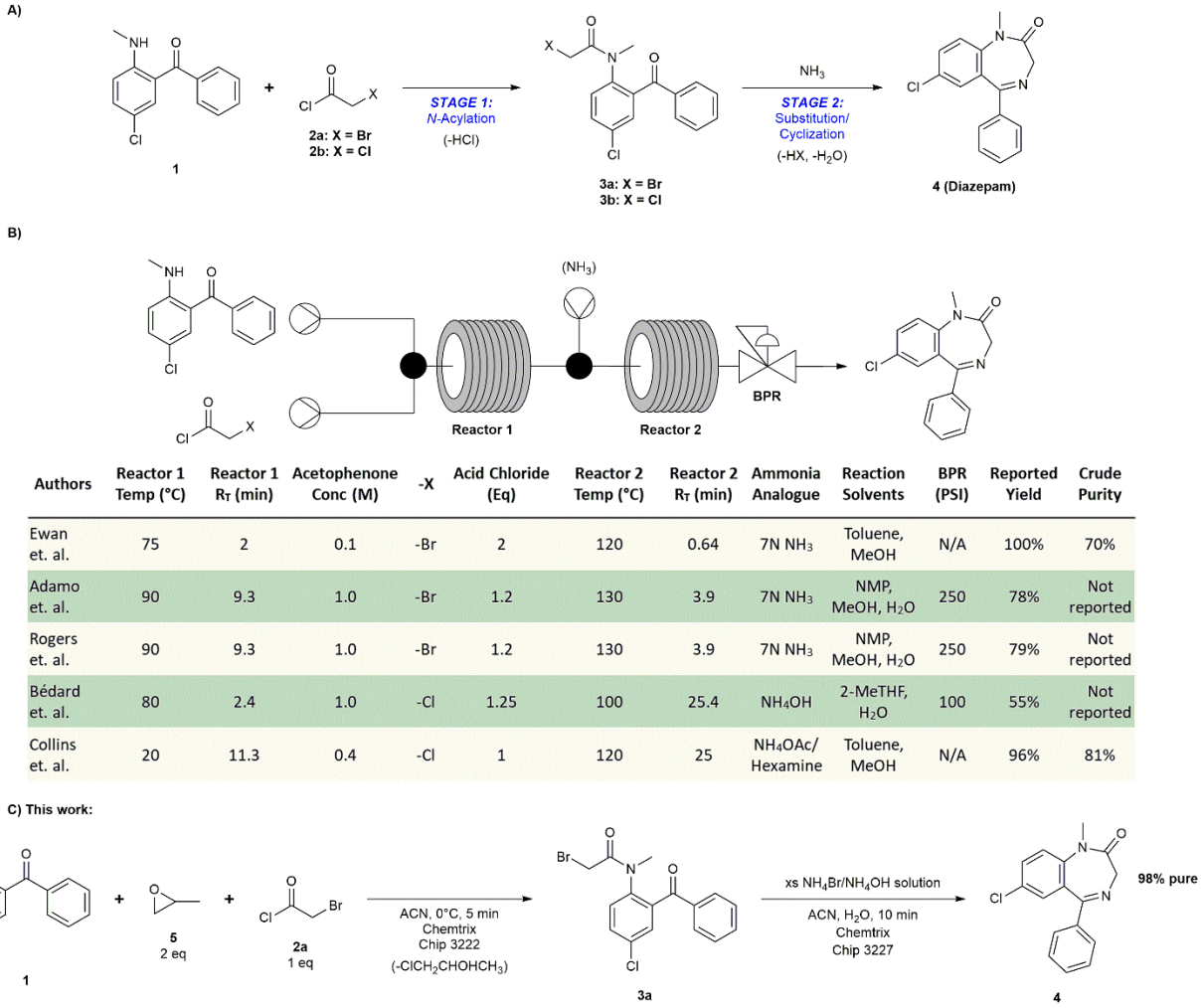

Authors	Reactor 1 Temp (°C)	Reactor 1 R_T (min)	Acetophenone Conc (M)	-X	Acid Chloride (Eq)	Reactor 2 Temp (°C)	Reactor 2 R_T (min)	Ammonia Analogue	Reaction Solvents	BPR (PSI)	Reported Yield	Crude Purity
Ewan et. al.	75	2	0.1	-Br	2	120	0.64	7N NH_3	Toluene, MeOH	N/A	100%	70%
Adamo et. al.	90	9.3	1.0	-Br	1.2	130	3.9	7N NH_3	NMP, MeOH, H_2O	250	78%	Not reported
Rogers et. al.	90	9.3	1.0	-Br	1.2	130	3.9	7N NH_3	NMP, MeOH, H_2O	250	79%	Not reported
Bédard et. al.	80	2.4	1.0	-Cl	1.25	100	25.4	NH_4OH	2-MeTHF, H_2O	100	55%	Not reported
Collins et. al.	20	11.3	0.4	-Cl	1	120	25	NH_4OAc/ Hexamine	Toluene, MeOH	N/A	96%	81%

Figure 2.1 Summary of the transformation of 5-chloro-2-(methylamino)benzophenone to diazepam. A) Scheme of the two-step synthesis of diazepam 4 from benzophenone 1. N-Acylation with an acid chloride occurs in Stage 1. Stage 2 includes a nucleophilic substitution with ammonia followed by an intramolecular cyclization. B) Summary of relevant literature where authors performed a two-step diazepam synthesis in continuous flow. C) Scheme of our optimized synthesis of diazepam in flow 49 where we obtained highly pure API directly from the process stream.

Given the wide range of yields and purities, we anticipated that there was potential to improve upon the published flow syntheses for diazepam. Ewan *et al.* and Collins *et al.* both report high yields; however, their impurity profiles indicate that intermediate **3a**/**b** did not fully react and was present in their final products. Rogers *et al.* noted that the downstream liquid-liquid extraction work-up led to yield deterioration since the product adsorbed to the membranes of the in-line phase separators. We sought to maximize starting material and intermediate conversion to produce a high quality API by increasing recovery from a simplified work-up. For this reason, we wanted to avoid

high boiling protic solvents since many of them are miscible with water and require high energy inputs for their removal by distillation. While it was not a top priority, we also considered methods for improving the safety of the flow process. Amination reactions in flow are commonly performed with 7N NH_3 in MeOH at high temperatures. Ammonia vapors will escape unless the system is kept under high pressure,[20] thus posing a potential manufacturing safety risk upon process upscaling.

With these considerations in mind, we sought to improve upon the reported methods by optimizing parameters such as retention time, temperature, solvent, and ammonia source using Chemtrix microfluidic chip reactors. We also evaluated methods for increasing reaction rates and improving chemoselectivity. The inclusion of propylene oxide as an HCl scavenger in Stage 1 improved the conversion of **1** into **3a** instead of the less reactive side product **3b**. We also discovered that saturated solutions of NH_4Br dissolved in 30% NH_4OH were able to convert **3a** into **4** using moderate temperatures without a back pressure regulator (BPR) (Figure 2.1c). As a result of these efforts, we were able to develop a more efficient and simplified telescoped process that fully converts **1** into 98% pure diazepam in 30% yield using a microscale system and up to 91% pure diazepam in 96% isolated yield with and upscaled system before final recrystallization in EtOH.

2.2 Methods

5-Chloro-2-(methylamino)benzophenone, propylene oxide, bromoacetyl chloride, 7N NH_3/MeOH solution, triethylamine (TEA), *N*,*N*-diisopropylethylamine (DIPEA), 1,8-diazabicyclo[5.4.0]undec-7-ene (DBU), 2,6-lutidine, Na_2CO_3, 28-30% NH_4OH solution, NH_4OAc, and NH_4Br were purchased from MilliporeSigma and were used without further purification. Diazepam HPLC standard was also obtained from MilliporeSigma and used as supplied. Toluene, ethyl acetate (EtOAc), *N*-methylpyrrolidone (NMP), ethanol (EtOH) and HPLC grade acetonitrile (ACN) were supplied by Fisher Scientific and used as received.

HPLC chromatograms were acquired using an Agilent 1200 Series HPLC with a G1315B Diode Array Detector. Samples were analyzed on a ZORBAX Eclipse XDB-18 column (5 µm particle size, 4.6 x 150 mm) at 20°C. The mobile phase consisted of a 40:40:20 ACN:H_2O:MeOH solvent system flowing at 0.5 mL/min. UPLC chromatograms were obtained using an Acquity UPLC H-class PLUS system with a CORTECS C18+ column (1.6 µm particles, 2.1 x 100 mm)

and an Acquity QDa Mass Detector for LC-MS. A 2.1 x 5 mm CORTECS VanGuard Pre-Column was installed preceding the analytical column. ^{1}H and ^{13}C NMR spectra were obtained using a Bruker Avance III-HD (500 MHz) instrument. Chemical shifts are reported using the residual solvent peak as reference. All microfluidics experiments were carried out using a Chemtrix Labtrix S1 system. Telescoped reactions used a Chemtrix Labtrix Start system as a second temperature-controlled stage. Each system was equipped with 3222 (5 μL), 3223 (10 μL), 3225 (10 μL), or 3227 (19.5 μL) reactor chips.

2.2.1 *N*-Acylation in Batch and Qualitative Analysis

Batch reactions were screened by adding 5-chloro-2-(methylamino)benzophenone (50 mg, 0.2035 mmol) to 4 mL vials with a stir bar and toluene or ACN (1.5 mL) as solvent. Solutions were allowed to stir in an ice bath (4°C), room temperature (23°C), or a heated oil bath (75°C). Once the solution temperature had equilibrated, 1 equivalent of base (TEA, DIPEA, DBU, or 2,6-lutidine) and 0, 1, 2, 4, or 8 equivalents of propylene oxide were added to solution. The reaction was initiated upon bromoacetyl chloride (32.1 mg, 0.2035 mmol) addition and allowed to stir for 15 minutes. Reactions were analyzed by TLC (2:1 petroleum ether:ethyl acetate) and HPLC.

2.2.2 Stage 1 Optimization in Flow

Solutions of 5-chloro-2-(methylamino)benzophenone (0.6 M), propylene oxide (1.2 M), and bromoacetyl chloride (0.6 M) were dissolved in toluene and loaded into three 1 mL Hamilton gastight syringes. A fourth syringe containing neat ACN was used for quenching. The filled syringes were mounted on the Labtrix S1 system and connected to the first three and second to last inlets of the chip holder by FEP tubing (0.8 x 0.25 mm).

Reactor chip 3225 was used for Stage 1 evaluation. Each condition was allowed to equilibrate for three times the retention time in an attempt to achieve steady-state before collection. Samples of 20 μL were collected in vials filled with 890 μL ACN and 100 μL of 0.25 M Na_2CO_3. Prior to UPLC analysis, samples were filtered through a 0.20 μm PTFE filter.

To optimize reagent stoichiometries, flow rates for the three reagents were initially set to 0.667 μL/min for 1.0 equivalents of bromoacetyl chloride. ACN wash flowed at a constant 1.00 μL/min throughout the run. As the bromoacetyl chloride equivalents increased by 0.02 increments,

the flow rate for the benzophenone and propylene oxide decreased by 0.004 μL/min. The rate for bromoacetyl chloride increased by 0.008 μL/min with each condition. This trend was carried throughout the screen until the flowrate for the benzophenone and propylene oxide was 0.625 μL/min and the bromoacetyl chloride was 0.750 μL/min for 1.2 equivalents of acid chloride. A table of this process is included in the Supplemental Information for clarity (Table 2.3). Residence time and temperature were held constant at 5 minutes and 0°C, respectively.

Residence times were then tested between 1 and 10 minutes at 1 minute increments. The flow rates for the starting reagents were each set to 3.33 μL/min for R_T = 1 min and decreased equally to give the appropriate residence time in the reactor until 10 minutes. An ACN quench was connected to the second to last port to dilute the reactant mixture by 50% v/v. Temperature was kept at 0°C unless stated otherwise.

2.2.3 Amination/Cyclization in Batch and Qualitative Analysis

Isolated intermediate **3a** was then used in batch to scout preferred ammonia sources. Vials were charged with **3a** (367 mg, 1.0 mmol) dissolved in 5 mL of solvent (toluene, ACN, or NMP) and different ammonia analogues, 7N NH_3 in MeOH (2 mL, 14 mmol), 28-30% NH_4OH (2 mL, ~29.6 mmol), 6 M NH_4OAc in water or MeOH (4 mL, 25.9 mmol), or a saturated solution of NH_4Br/NH_4OH (2 mL, 3.27 mmol) added to the vial. Reactions were performed at temperatures between room temperature and 100°C and allowed to react at various times between 15 minutes and overnight. Reactions were characterized by TLC or UPLC. Results are summarized in the Supplemental Information.

Intermediate **3a** was dissolved in toluene to give a 0.20 M solution that was loaded in a 1 mL syringe. Ammonia solutions were loaded into a second syringe. Syringes were mounted on the S1 system and fitted with FEP tubing leading to the first two inlets of the chip holder. Each sample obtained was separated by equilibration period set for three times the retention time of the condition about to be sampled.

In trials testing 7N NH_3 in MeOH, residence times (5-25 min) and temperatures (100, 120°C) were evaluated using reactor chip 3227. Flow rates for **3a**, 7N NH_3, and ACN quench were each set at 1.95 μL/min for 5 min down to 0.390 μL/min for 25 min. The system was fitted with a BPR set to 100 PSI. Solutions were collected in vials pre-filled with 225 μL ACN until 50 μL of product solution was collected and analyzed by UPLC.

The NH_4Br/NH_4OH solution was prepared by dissolving 5.1g NH_4Br in 1.36 mL NH_4OH solution and diluting to 12.5 mL with water. This solution and **3a** in toluene flowed at rates between 0.5 μL/min to 5 μL/min to achieve residence times of 1, 3, 5, or 10 minutes in reactor chip 3223 held at either 40°C and 60°C. The process flowed until 50 μL were dispensed into vials containing 500 μL ACN. Samples were immediately analyzed by UPLC and stored at -80°C.

2.2.4 Telescoped Synthesis of Diazepam in Flow

For experiments using NH_4OAc as an ammonia source, Stage 1 was fed solutions of 5-chloro-2-(methylamino)benzophenone (0.6 M), propylene oxide (1.2 M), and bromoacetyl chloride (0.6 M) in toluene at a rate of 0.667 μL/min (R_T = 5 min). Reactor chip 3225 (Stage 1) was cooled to 0°C and the contents from this stage flowed into reactor chip 3227. A solution of 6 M NH_4OAc dissolved in 100:0, 98:2, 95:5, or 90:10 MeOH:H_2O (v/v) was added at the second inlet of Stage 2 at a rate of 1.9 μL/min. The reactor was heated to 120-160°C using the Labtrix Start system. As NH_4OAc induced rapid gas formation, a BPR set to 100 PSI was added to the end of Stage 2. Fractions of 100 μL were collected for each solvent and temperature condition. A 10 μL aliquot of product was diluted in 100 μL ACN for UPLC analysis.

Our optimized telescoped process used ACN solutions of 5-chloro-2-(methylamino)benzophenone (0.15 M), propylene oxide (0.30 M), and bromoacetyl chloride (0.15 M) for Stage 1 and the NH_4Br/NH_4OH solution for Stage 2. Benzophenone and propylene oxide solutions mixed in an external T-mixer were fed into the first inlet of reactor chip 3222 where it mixed with the bromoacetyl chloride solution introduced via the second inlet. Flow rates for the three reagents in Stage 1 were 0.333 μL/min giving a residence time of 5 minutes. The output of this reactor was fed into reactor chip 3227 held at 60°C. A NH_4Br/NH_4OH solution was flowed into the chip at 0.95 μL/min to produce a residence time of 10 minutes for Stage 2 (no BPR was installed). Fractions were collected for 1 hour and analyzed by UPLC after diluting a 100 μL aliquot up to 1000 μL ACN. Diazepam concentrations in the final solutions were calculated based on a UPLC standard curve.

The optimized microfluidics system was converted into a larger scale setup where FEP tubing with an inner diameter of 1.016 mm was used. Solutions of 5-chloro-2-(methylamino)benzophenone (0.15 M), propylene oxide (0.30 M), and bromoacetyl chloride (0.15 M) were loaded into 6 mL syringes and positioned onto syringe pumps. The benzophenone and

propylene oxide were each pumped at a rate of 10 μL/min and mixed through a T-mixer. The mixed solution flowed into a subsequent T-mixer where it would mix with the bromoacetyl chloride solution also being pumped at 10 μL/min. The reactor tubing for stage one (R_T = 5 min, length = 18.5 cm) was submerged into an ice bath. The output of Stage 1 was fed into a final T-mixer immersed in a 60°C water bath where the NH_4Br/NH_4OH solution was introduced at 30 μL/min via a 10 mL syringe pump. The coiled tubing of Stage 2 (R_T = 5 min, length = 18.5 cm) sat in the heated water bath and deposited the final solution into a 20 mL scintillation vial. Fractions were collected in 1 hour increments. Solutions were worked up by EtOAc extraction and the solvent was removed *in vacuo*.

2.3 Results and Discussion

2.3.1 *N*-Acylation Optimization in Batch

Our initial efforts were focused on developing a deeper understanding of both reactions. In the *N*-acylation step (Figure 2.2a), **1** will attack **2a** to give **3a** in a nucleophilic acyl substitution by the secondary amine of **1**. An ammonium intermediate is formed with subsequent deprotonation of the intermediate by chloride to generate **3a** and HCl as products. It is important to note that deprotonation by unreacted **1** competes with chloride in this process and acts as a buffer for the HCl by-product in the reaction. In either case (Figure 2.2b), the nucleophilicity of **1** is decreased, thus impeding reaction progress. A common strategy to offset this limitation is to increase the equivalence of the amine; however, given our goals of maximizing conversion in flow, this was not an option as it would increase E-factor by requiring more starting material and a downstream purification that could negatively impact product yield.

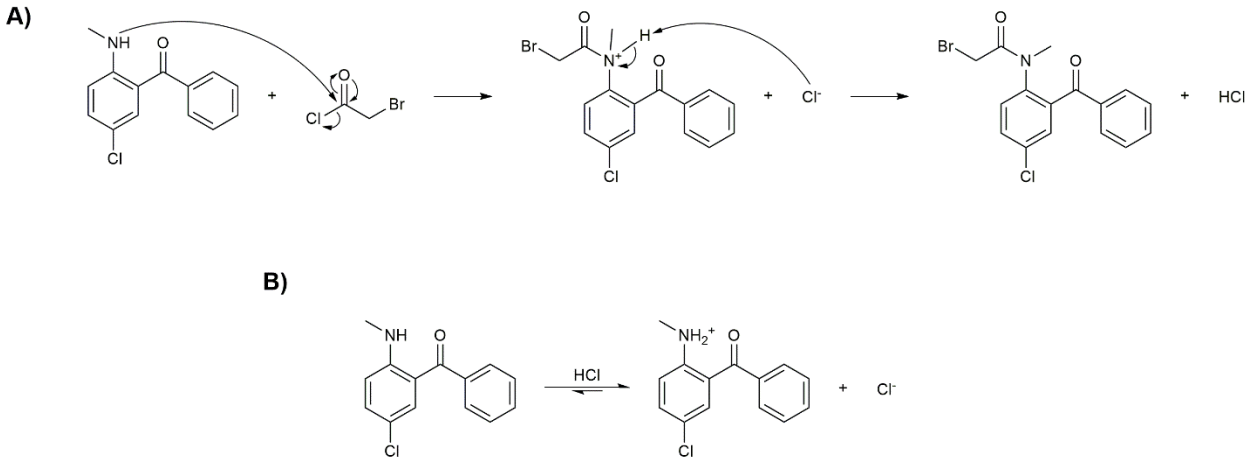

Figure 2.2 Microscopic steps associated with the N-acylation of Stage 1. A) Mechanism of the intended reaction with 1 and 2a, generating HCl along with the desired intermediate 3a. B) Unreacted 1 can be protonated by generated HCl, a strong electrolyte, or other protonated ammonium intermediate, thereby reducing the rate of the intended reaction.

We initially thought that adding a bulky base to the reaction could quench the generated HCl and facilitate the acylation. After evaluating a variety of bases (triethylamine, DIPEA, DBU, and 2,6-lutidine) in 15 minute batch reactions at different temperatures, we found that they inhibited the formation of **3a** and promoted the formation of **3b** (Table 1). A plausible explanation for this is that under basic conditions, the nucleophilicity of chloride increases and substitutes at the α-bromide on **3a**. When looking at temperature as a variable, we generally observed the formation of the chloride intermediate **3b** at elevated temperatures in both the presence and absence of base. It is possible to drive **3b** to diazepam as Bédard *et al.* and Collins *et al.* have shown; however, we have a preference for the bromide analogue **3a** since the subsequent cyclization reaction is much more facile with this species. In fact, under a wide variety of conditions tested that fully consumed **3a**, the **3b** concentrations remained virtually unchanged in the reaction mixture. Since base addition did not improve conversion into the desired **3a** intermediate, we then explored the effects of temperature and additives on reaction efficiency.

Table 2.1 Peak areas of key compounds as determined by HPLC. The control conditions where there was no base had the best conversion into **3a** as opposed to any of the reactions with base present. Lower temperatures generally seem to improve conversion rates into **3a**.

Condition	*0°C*	*23°C*	*75°C*	*0°C*	*23°C*	*75°C*	*0°C*	*23°C*	*75°C*
No base	83.17	49.07	81.90	16.80	40.65	9.20	0	0.48	6.88
TEA	28.44	3.59	40.06	14.24	32.72	41.28	38.29	43.75	16.42
DIPEA	18.32	3.39	14.44	38.44	38.22	56.71	63.57	55.25	27.28
DBU	6.04	7.24	17.02	64.27	47.32	48.69	27.53	44.42	33.35
2,6-Lutidine	24.81	11.02	20.62	23.51	58.91	65.26	25.13	14.24	0

While investigating alternative methods to improve the *N*-acylation reaction, we began to explore the use of propylene oxide as an auxiliary species. Balaji and Dalal[21] have reported rapid conversion of primary and secondary amine derivatives into amides using propylene oxide as a neutral HCl scavenger. Propylene oxide has been used specifically for the purpose of quenching HCl in reactions to form 1- and 2-chloropropanols;[22] the chlorohydrin by-products were benign spectators in those reactions as well.[23] No reports of propylene oxide use in any benzodiazepine synthesis exist to our knowledge.

In Stage 1 batch reactions with different equivalents of propylene oxide, we found that the conversion of **1** to **3a** was increased significantly. As shown in Figure 2.3, addition of one equivalent of propylene oxide led to a **3a** yield improvement from 83% to 91% and a more complete conversion of **1** (8.6% vs. 1.2% for the two trials). Notably, the amount of **3b** side-product also decreases slightly as the propylene oxide equivalents increased. Since the increased reaction rate with propylene oxide offered the opportunity to reduce the residence time of Stage 1 in flow while promoting better **3a** vs. **3b** selectivity, all subsequent experiments used two equivalents of propylene oxide as the best compromise between reaction yield vs. reagent consumed.

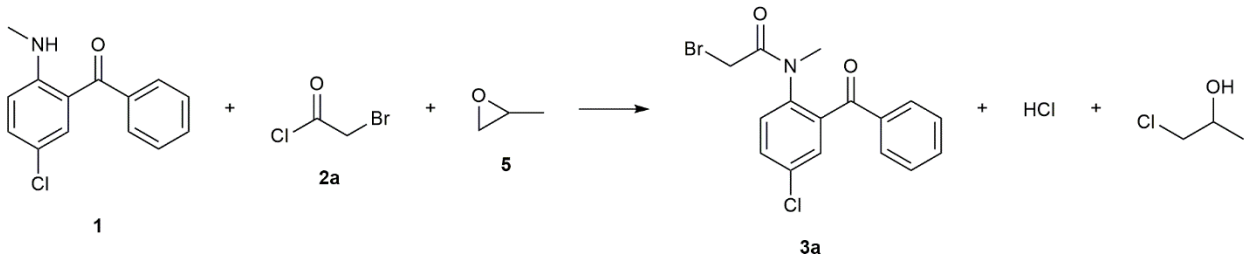

Propylene Oxide Equiv.	% **3a**	% **3b**	% **1**
0	82.98	7.58	8.64
1	91.37	6.68	1.17
2	94.57	4.69	0
4	92.55	3.21	3.65
8	92.84	3.34	3.06

Figure 2.3 Summary of propylene oxide screen in batch. Propylene oxide (5) was added to the above reaction at different equivalencies. It was found that propylene oxide plays a role in converting starting material into the resulting amide more efficiently.

2.3.2 Stage 1 Optimization in Flow

With the above conditions above in hand, we were able to translate the batch *N*-acylation reaction into flow using a Chemtrix Labtrix S1 system to operate at a milligram scale for flow rate, equivalence, and temperature optimization efforts. Solutions of **1**, **5**, and **2a** were dissolved in toluene to give solutions of 0.6 M, 1.2 M, and 0.6 M, respectively, loaded into 1 mL syringes, and mounted on the S1 system. The flow rate of each reagent was adjusted to rapidly test different concentrations of **2a** at increments of 0.02 equivalents between 1.0 – 1.2 equivalents. We initially conducted this experiment with a 10 minute residence time; however, we observed that the *N*-acylation reaction reached completion for all trials tested between 1.0 - 1.1 equivalents (Supplemental Information) thus warranting a shorter retention time.

Next, we ran 3 trials of this optimization experiment with a R_T = 5 min, where each trial was conducted on different days by different operators (Figure 2.4) and found high conversions into intermediate **3a** with a majority of the starting material being consumed even using 1.0 equivalents of **1**. Since the peak areas stay fairly consistent as the amount of **2a** increases with only minor fluctuations, we concluded that the *N*-acylation reaction is reaching completion within 5 minutes under these conditions.

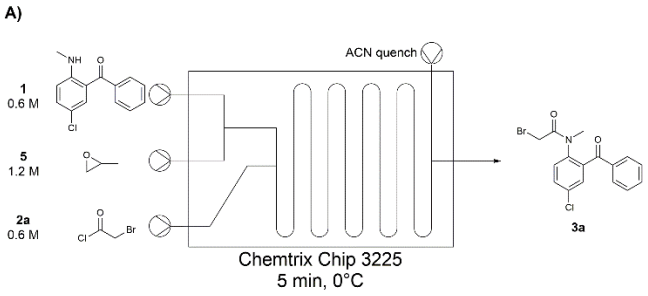

Equivalents of **2a**	% **3a**	% **3b**	% **1**
1.00	91.09 ± 1.57	1.95 ± 0.15	3.62 ± 0.87
1.02	94.62 ± 1.61	2.01 ± 0.05	0.92 ± 0.92
1.04	91.65 ± 2.69	1.80 ± 0.09	4.21 ± 3.40
1.06	93.97 ± 0.33	1.88 ± 0.02	0.70 ± 0.19
1.08	95.68 ± 0.43	1.96 ± 0.09	0.50 ± 0.05
1.10	95.10 ± 0.31	1.93 ± 0.04	0.18 ± 0.18
1.12	95.79 ± 0.02	1.92 ± 0.01	0.11 ± 0.11
1.14	95.83 ± 0.26	1.70 ± 0.15	0.00 ± 0.00
1.16	89.37 ± 6.34	2.29 ± 0.56	1.60 ± 1.60
1.18	93.26 ± 6.74	1.49 ± 1.49	0.17 ± 0.17
1.2	91.85 ± 1.44	3.28 ± 0.50	2.22 ± 2.22

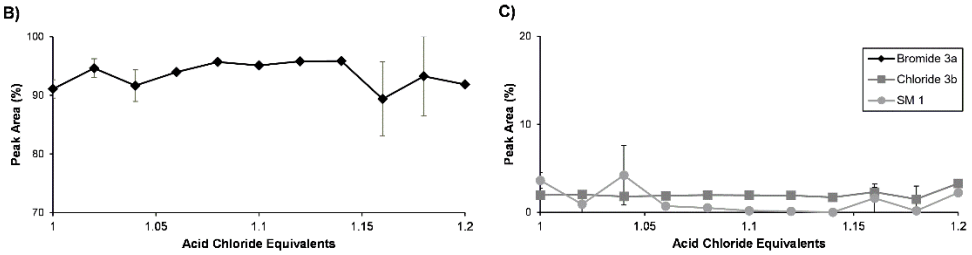

Figure 2.4 Summary of acid chloride stoichiometry optimization in toluene in Stage 1. A) Setup for reaction screen in microfluidic reactor with tabulated results. B) Plot of results with standard error from 3 trials.

We then sought to determine the optimal residence time for Stage 1 at this stoichiometry (Figure 2.5). Using the same flow setup as before, we were able to test 1-10 min residence times at 1-minute intervals. We found that the *N*-acylation is fast at 0°C, such that the majority of starting material **1** is consumed within 1 minute. There is a gradual increase in the amount of bromide intermediate **3a** up until the 5-to-6-minute mark where the amount of product plateaus as time progresses. The amount of **1** present also reaches a minimum at 5 minutes; however, **3a** slightly decreases at residence times ≥ 7 minutes due to formation of **3b** or a reverse reaction that converts the intermediate back into starting material **1**. Based on an average of three trials, the chloride intermediate **3b** stays relatively constant at 2-3%. Given that the maximum conversion from **1** to **3a** at 5 minutes, we moved forward with a 1:1:2 ratio of **1**:**2a**:**5** and a R_T = 5 min at 0°C as our optimized results for Stage 1.

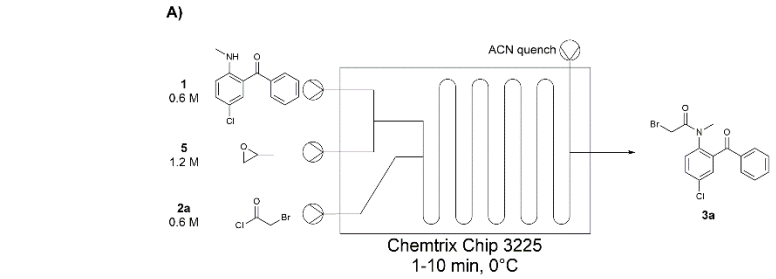

Retention Time (min)	% 3a	% 3b	% 1
1	83.19 ± 3.27	1.85 ± 0.17	12.80 ± 3.59
2	87.12 ± 1.16	4.49 ± 2.76	6.26 ± 3.07
3	88.89 ± 0.63	3.72 ± 1.96	4.86 ± 2.41
4	91.21 ± 1.56	3.40 ± 1.58	3.60 ± 2.33
5	94.84 ± 2.28	1.96 ± 0.16	0.56 ± 2.20
6	94.41 ± 0.26	2.06 ± 0.05	0.71 ± 0.56
7	90.76 ± 0.64	2.96 ± 0.15	0.64 ± 0.71
8	91.37 ± 3.81	3.94 ± 0.44	0.81 ± 0.64
9	89.18 ± 2.53	2.83 ± 1.03	1.43 ± 0.81
10	91.79 ± 3.75	3.02 ± 0.18	1.15 ± 0.54

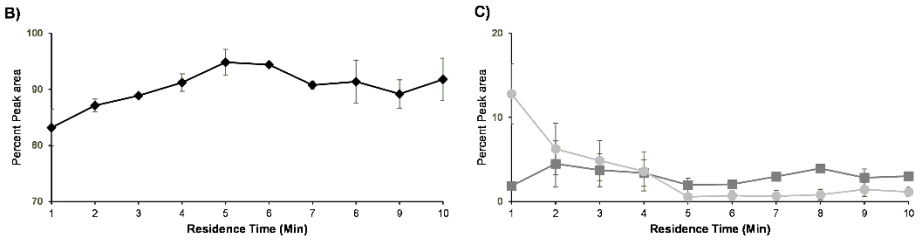

Figure 2.5 Summary of residence time optimization in toluene in Stage 1. A) Setup for reaction screen in microfluidic reactor with tabulated results. B) Plot of results with standard error from 3 trials.

2.3.3 Stage 2 Cyclization and the Search for an Improved Ammonia Source

NH_3

The mechanism of the Stage 2 process (Figure 2.6) begins with a nucleophilic displacement of bromide from **3a** by an ammonia molecule in an S_N2 reaction that generates HBr as a by-product. The α-amino intermediate then condenses with the ketone to form an imine to give diazepam. Since the HBr and H_2O by-products can potentially drive acid hydrolysis of the amide bond of **3a** to regenerate the starting material, it is necessary for ammonia to substitute the bromine and quickly undergo cyclization to form diazepam. This transformation appears to be the rate-limiting step in diazepam synthesis given the high temperatures reported in the previously cited literature.

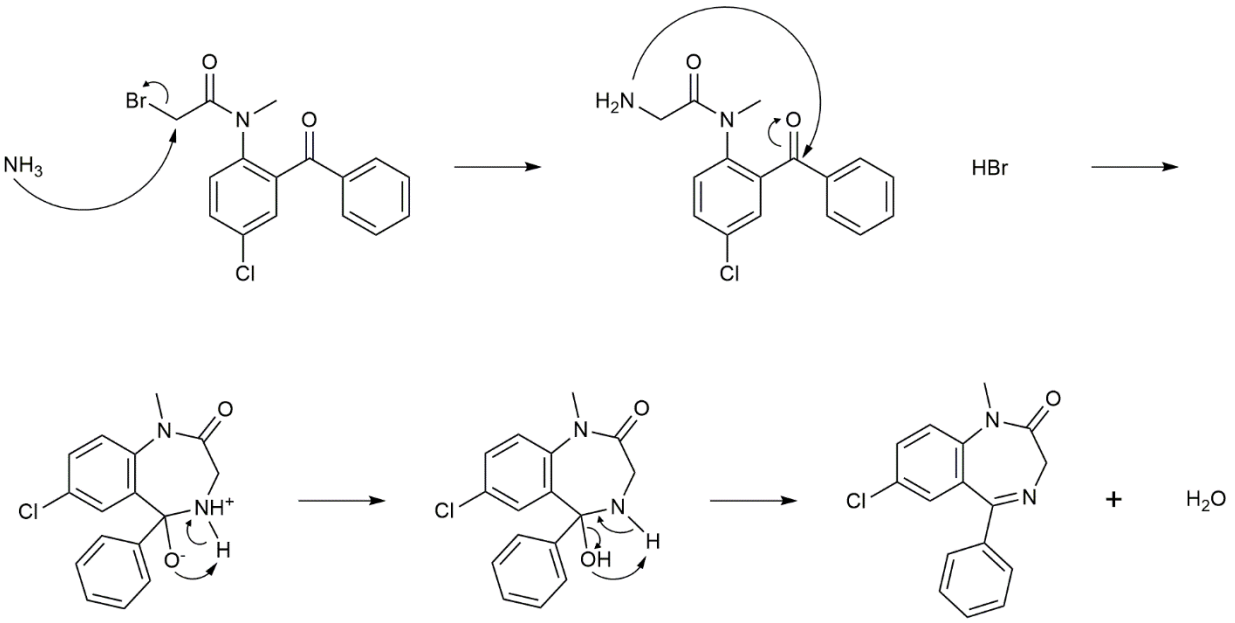

Figure 2.6 Mechanism associated with the substitution and subsequent cyclization in Stage 2. Ammonia displaces bromide before engaging in an intramolecular attack of the ketone to form a 7-membered ring. Loss of water from the intermediate oxonium ion leads to imine formation of diazepam along with HBr and H_2O.

This analysis led us to identify the most favorable ammonia source given the variety of analogues described in the literature. Our first candidate was ammonia dissolved in methanol used by Ewan *et al.*, Adamo *et al.*, and Rogers *et al.* We conducted Stage 2 batch reactions with isolated intermediate **3a** and 7N NH_3 in MeOH. Due to pressure built-up from the ammonia and low boiling MeOH, we conducted this reaction at 65°C. Although diazepam formation was observed, the presence of **1** was also detected by HPLC indicating that these conditions can induce hydrolysis of the amide bond.

We moved our operations to flow where we could reproduce the conditions as described by Ewan *et al.* and Rogers *et al.* We first set out to evaluate Stage 2 at different residence times from 5 to 25 minutes at 100°C and 120°C using a 0.2 M solution of **3a** in toluene (Figure 2.7). A BPR was installed to maintain an internal pressure of 100 PSI. These trials were successful in producing diazepam; however, the material collected was slightly yellow, a by-product formed during Stage 2 that was identified by UPLC as the hydrolysis product **1**. This impurity was produced at various quantities depending on the flow conditions employed. Given this drawback and the need for a highly pressurized system, we were motivated to investigate alternative ammonia sources.

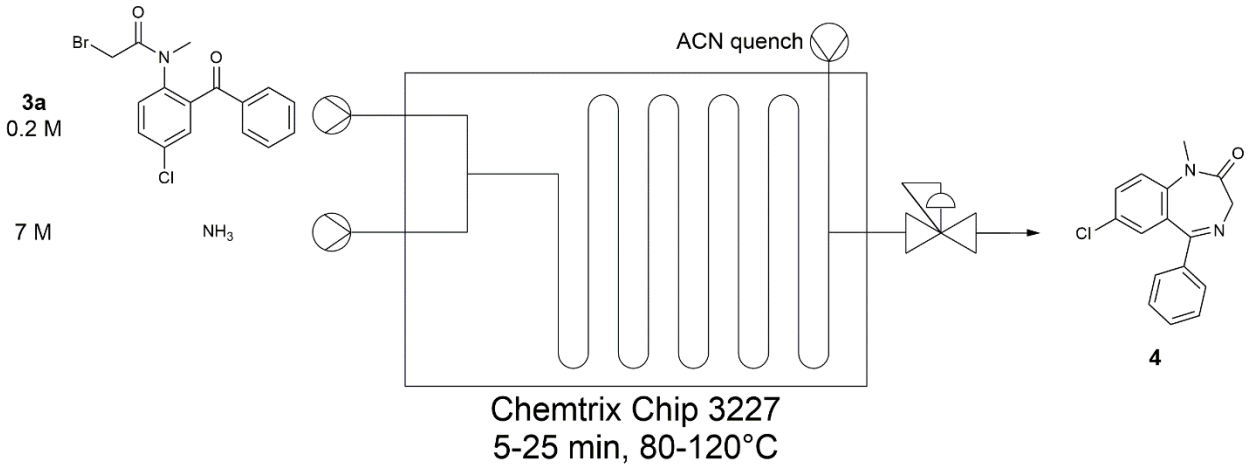

	% 4					% 1				
Time	*5 min*	*10 min*	*15 min*	*20 min*	*25 min*	*5 min*	*10 min*	*15 min*	*20 min*	*25 min*
100°C	78.28	94.17	85.38	88.11	90.19	95.24	91.48	88.42	89.58	92.76
120°C	7.88	4.27	14.62	11.89	9.81	3.78	7.00	10.10	10.00	5.61

Figure 2.7 Summary of temperature and residence time trials for NH_3 in Stage 2. Intermediate **3a** was dissolved in toluene whereas NH_3 was dissolved in MeOH. The BPR was set to 100 PSI.

NH_4OH

Reactions conducted at 70°C with **3a** and NH_4OH dissolved in a toluene / ACN mixture also produced diazepam; however, a significant portion of **3a** reverted back to benzophenone **1** based on UPLC analysis. While this had potential for being a viable ammonia source, especially with the work by Collins *et al.* supporting this reagent, we chose not to investigate this ammonia analogue further in flow due to the impact that the intermediate hydrolysis would have on the process E-factor.

NH_4OAc

We then pursued the use of an aqueous solution of NH_4OAc in an effort to suppress the competition between hydrolysis and cyclization. By keeping the reaction closer to a neutral pH, we reasoned that the hydrolysis rate might be reduced enough to enable intermediate conversion into diazepam before the amide bond cleaves. We first carried out reactions with NH_4OAc as the ammonia source in batch with a variety of solvents, including ACN, NMP, and toluene, in a one-pot reaction with benzophenone **1** as the starting reactant. When ACN was the solvent, we obtained

a crude purity of 87% diazepam that could be readily crystallized to 95% pure API. Given the promise of the NH_4OAc reagent, we moved on to flow trials.

For the flow experiments, we made a 6 M solution of NH_4OAc in MeOH and mixed it with the Stage 1 product in Stage 2 while varying temperature between 120-160°C at 10°C intervals (Figure 2.8). With a fixed residence time of 5 minutes, we observed 50% or more diazepam in the crude product, although a significant amount of **1** and another prominent peak that eluted near the toluene peak was observed. UPLC-MS analysis revealed that the new peak had an *m/z* value of 346 without an accompanying M+2 peak, indicative of an acetate adduct arising from bromine displacement (Supplemental Information). Flash chromatographic isolation of this impurity and characterization by ^{1}H and ^{13}C NMR confirmed this structure (Supplemental Information). While acetate is not a particularly strong nucleophile, we suspected that the abundance of this anion in the reaction mixture could promote displacement at the halogenated α-carbon. In an effort to suppress the amount of the acetate adduct formed, we increased the water content in the 6 M solutions of NH_4OAc using 2%, 5%, and 10% water in MeOH by volume; however, these efforts proved fruitless.

A)

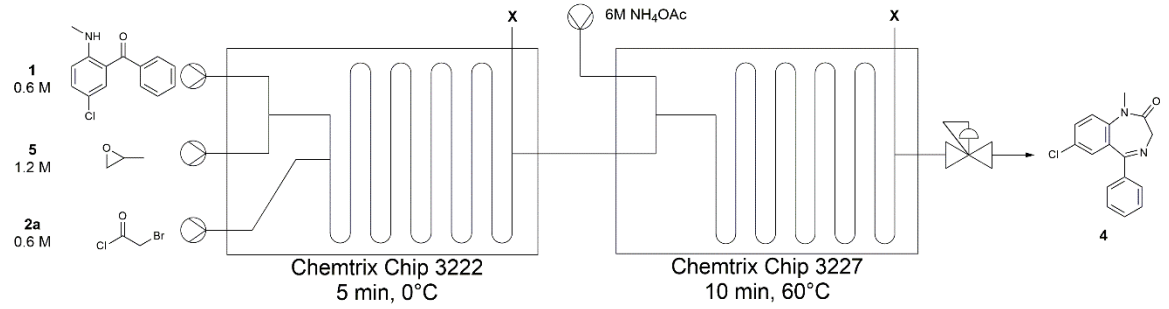

	% 4					% 6				
Condition	*120°C*	*130°C*	*140°C*	*150°C*	*160°C*	*120°C*	*130°C*	*140°C*	*150°C*	*160°C*
0% H_2O	50.48	46.90	30.72	27.60	14.56	16.50	10.52	6.75	21.07	5.29
2% H_2O	34.68	38.90	2.95	2.48	2.53	15.68	9.90	1.04	0.32	0.28
5% H_2O	59.22	64.65	53.65	28.87	26.76	15.10	21.36	14.54	22.85	17.01
10% H_2O	56.40	57.67	37.52	26.37	28.39	22.75	20.52	27.20	29.7	19.05

B)

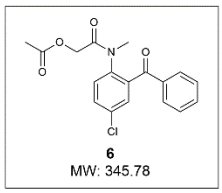

Figure 2.8 Summary of Stage 2 temperature and NH_4OH solvent screen in telescoped synthesis of diazepam. A) Setup for reaction screen in microfluidic reactor with tabulated results. Starting materials were dissolved in toluene. NH_4OH was dissolved in MeOH with 0%, 2%, 5%, or 10% water to give 6M. BPR was set to 100 PSI. B) Proposed impurity that arises from reaction conditions with NH_4OAc.

NH_4Br/NH_4OH

The formation of the acetate adduct made us focus on the role the spectator ion plays in the reaction. Knowing that the acetate has the ability to substitute the halogenated α-carbon, we decided to incorporate NH_4Br in the case that if the common bromide ion were to act as a nucleophile, it would be a zero sum reaction. We dissolved the salt in an aqueous NH_4OH solution to serve as our primary source of ammonia via a common ion effect to drive the formation of NH_3 as shown in Figure 2.9. Since NH_4Br dissociates into NH_4^+ and Br^- ions and NH_4OH is in equilibrium with NH_4^+ and OH^-, NH_4^+ is a common ion, thus shifting the equilibrium of NH_4OH towards NH_3 and water.

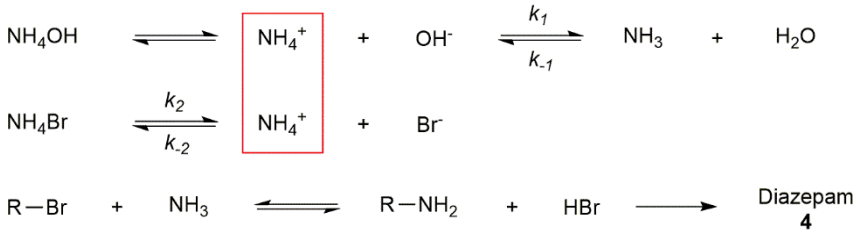

Figure 2.9 Relevant equilibria for the NH_4Br/NH_4OH ammonia surrogate system. Note that NH_4Br and NH_4OH will dissociate and share NH_4^+ as a common ion. Since NH_4Br is a strong electrolyte, the higher concentration of NH_4^+ generated will drive equilibrium towards NH_3. This higher equivalence of NH_3 appears to drive the formation of **4** from the intermediate **3a**. Constants: $k_{-1} = 1.76*10^{-5}$. $k_2 = 25.5$.

Preliminary batch trials with the NH_4Br/NH_4OH solution for cyclization demonstrated that we could achieve excellent conversion of **3a** into diazepam within 2.5 hours. UPLC of the crude revealed 73% and 90% diazepam at room temperature and 40°C, respectively. Performing a one-pot reaction from **1** to **4** generated 94% diazepam when using NH_4Br/NH_4OH in an overnight reaction. In all trials attempted in flow, we observed little or no **1** by-product and traces of **3b** arising from Stage 1.

Subsequent flow experiments with NH_4Br/NH_4OH in Stage 2 employed **3a** in ACN (Figure 2.10). We transitioned to this solvent since batch experiments revealed that toluene slows down the reaction, likely due to its immiscibility with water and its inability to dissolve NH_4Br or NH_4OH. During our residence time screening campaign, we realized that a BPR was no longer necessary for the reactor system, so it was removed. At 40°C, we were able to observe crude yield

of diazepam as high as 61% after 10 minutes and the yield improved to 86% diazepam when the temperature was increased to 60°C.

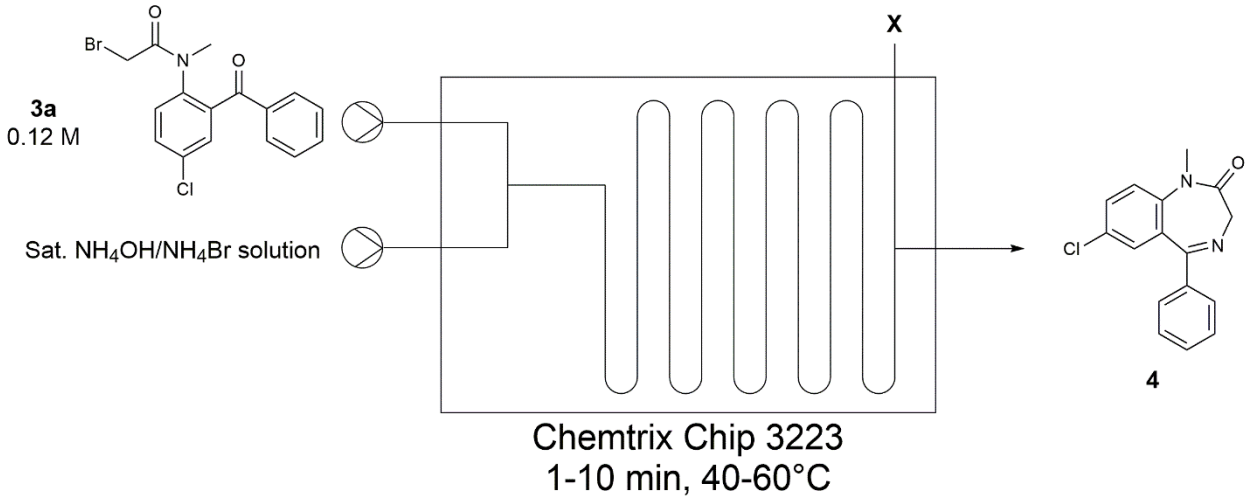

Time (min)	% 4		% 3a	
	40°C	*60°C*	*40°C*	*60°C*
1	5.42	17.43	90.06	76.10
3	5.42	47.91	90.06	44.96
5	32.21	65.05	57.53	27.62
10	61.24	85.93	28.53	4.63

Figure 2.10 Summary of temperature and residence time trials using NH_4OH/NH_4Br solution in Stage 2. Intermediate **3a** was dissolved in ACN, while NH_4OH/NH_4Br solution was dissolved in water.

With a promising ammonia source in hand, we moved forward with optimization of the telescoped sequence as shown in Figure 2.11a. The first reactor chip was set for a 5 minute residence time at 0°C. As for Stage 2, we used a Chemtrix reactor chip 3227 heated to 60°C with a residence time of 10 minutes. Early attempts of telescoping this reaction in flow saw varying degrees of success that were primarily dictated by the buildup of a dark brown precipitate in Stage 2 where the NH_4Br/NH_4OH solution mixes with the reactant solution in the narrow channels of the static mixer in the chip (Figure 2.11b). This was unexpected, but not unusual, as Ewan *et al.* and Bédard *et al.* report a precipitate forming at a similar position. We were able to isolate enough of the precipitate to identify it as diazepam based on the similarity in UPLC retention times relative

to diazepam standard. (Supplementary Information). The solid could be easily removed using dilute acid which is another indicator of its identity as diazepam is readily soluble in acidic mediums. Given these observations, we inferred that the diazepam is formed instantaneously in the mixing element and forms a salt precipitate with residual HCl.

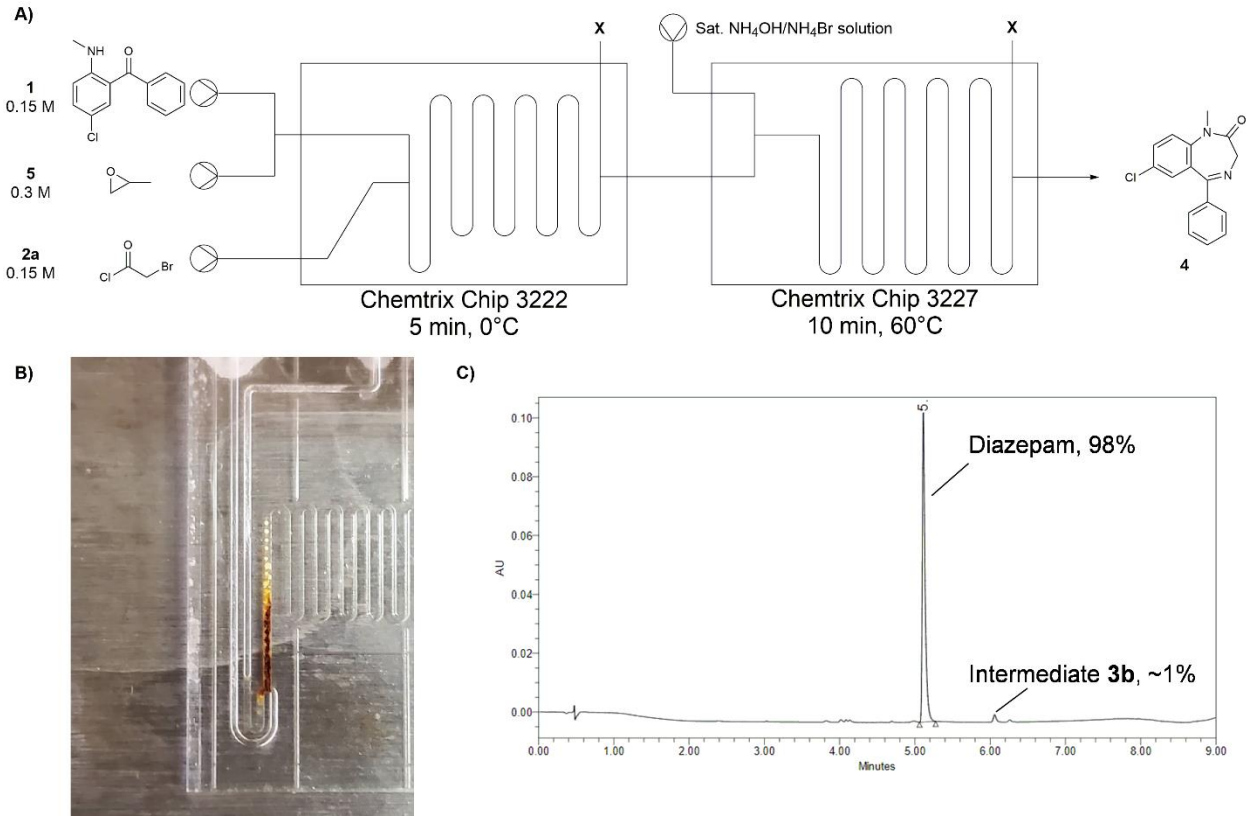

Figure 2.11 Summary of finalized telescoped flow process to synthesize diazepam in two-steps. A) Setup for two-step reaction in microfluidic reactor with tabulated results. Starting materials were dissolved in ACN. The NH_4OH/NH_4Br solution was dissolved in water. B) Precipitate thought to be diazepam crashes out at the point where the ammonia analogue enters the system. Sonication reduces the amount of precipitation that is formed here. C) Chromatogram of a fraction collected over 60 minutes to give 30% diazepam with a purity of 98%. Retention times: 5.1 min = diazepam, 6.0 min = chloride intermediate **3b**.

The solution Bédard *et al.* used to overcome this issue was sonication of the T-mixer where the ammonia source was added. We initially tried this remedy by submerging the second reactor into a bath sonicator heated to 60°C. This appeared to have helped our precipitation problem as our conversions substantially improved. Our best fraction from the telescoped trials without sonication was 86% pure diazepam. With sonication, we were able to consistently obtain 98% pure

diazepam across multiple 30 minute fractions (Figure 12c), although we still observed some precipitation buildup as before. Sonication also boosted conversion of the chloride impurity **3b** that was inert under our previous conditions. Analyzing the sonicated solutions against a calibration curve, it was found that we obtained approximately a 30% yield over the course of 1 hour in the sonicated system. We hypothesize that the sonication, while able to accelerate the reaction, is not as sufficient in fully dissolving diazepam and may allow crystallization to occur on the inner walls of the reactor channels. We investigated a few different strategies to prevent or at least reduce precipitation such as changing the solvent composition, but regardless of what we tried still resulted in clogging. We were eventually led towards using a larger scaled system as the higher flowrates and larger bore sizes could mitigate the issues with yield stemming from this precipitation problem. Using the setup described in the Methods section and Supplemental Information, this approach proved to be a useful as the solid effectively passed through the system to the point where no buildup was observed.

We took advantage of the scaled system to collect multiple 1 hour factions of material. The crude fractions had purities up to 91% diazepam with minimal optimization at this scale. Unlike the microscale, we were easily able to perform work-ups with EtOAc and aqueous washes where we were able to obtain yields by mass averaging to about 96%, a significant improvement from a 30% yield. We were also able to perform a single recrystallization with these acquired solids using EtOH improving the purity of collected diazepam to 98% and above. These findings demonstrate the viability and scalability of our conditions discovered in microfluidics for upscaled production without worry of clogging by precipitation. Minor optimizations at this scale, or potentially scales even larger, can be performed to increase diazepam purity and yield even further thus making this a viable system for diazepam production.

2.4 Conclusion

To conclude, we have been able to build upon previous work in the literature to intensify the production of diazepam in continuous flow achieving high crude purities using propylene oxide as an HCl scavenger and NH_4Br/NH_4OH as an alternative ammonia source to improve yield and purity while decreasing reactor temperatures. While possible to perform the two-step process on a microscale system, diazepam crashing out of solution prevented the yield from exceeding 30%. It was only when we shifted to a larger system that we could finally achieve satisfactory yields of

96%. This scaling effort simultaneously demonstrates the robustness of our system as we were able to maintain high crude purities just as on the microscale. The benefit of focusing on a high purity is the reduced solvent consumption for purification, reduced labor costs, and improve E-factor. Since diazepam is a member of a large family of 1,4-benzodiazepine derivatives, we anticipate that this work may serve as a foundation to synthesize other benzodiazepines in continuous flow to continue the ongoing effort to strengthen the supply chains of essential medicines.

2.5 Supplementary Information

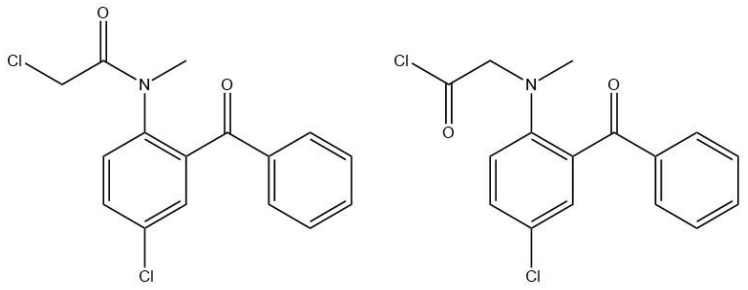

Figure 2.12 Structures of the two possible chloride impurities. Structure 3b results from an N-acylation of chloroacetyl chloride or bromoacetyl chloride where the bromide is substituted by a free chloride in a secondary reaction. Structure **7** is the proposed structure of the S_N2 reaction at the α-bromide resulting in an acid chloride intermediate.

Protocol for the synthesis of **3b**: 5-chloro-2-(methylamino)benzophenone (0.369 g, 1.5 mmol), chloroacetyl chloride (0.152 mL, 1.5 mmol), and propylene oxide (0.210 mL, 3.0 mmol) were added to a round bottom flask with 30 mL ACN and stir bar. Reaction stirred at room temperature for 30 minutes.

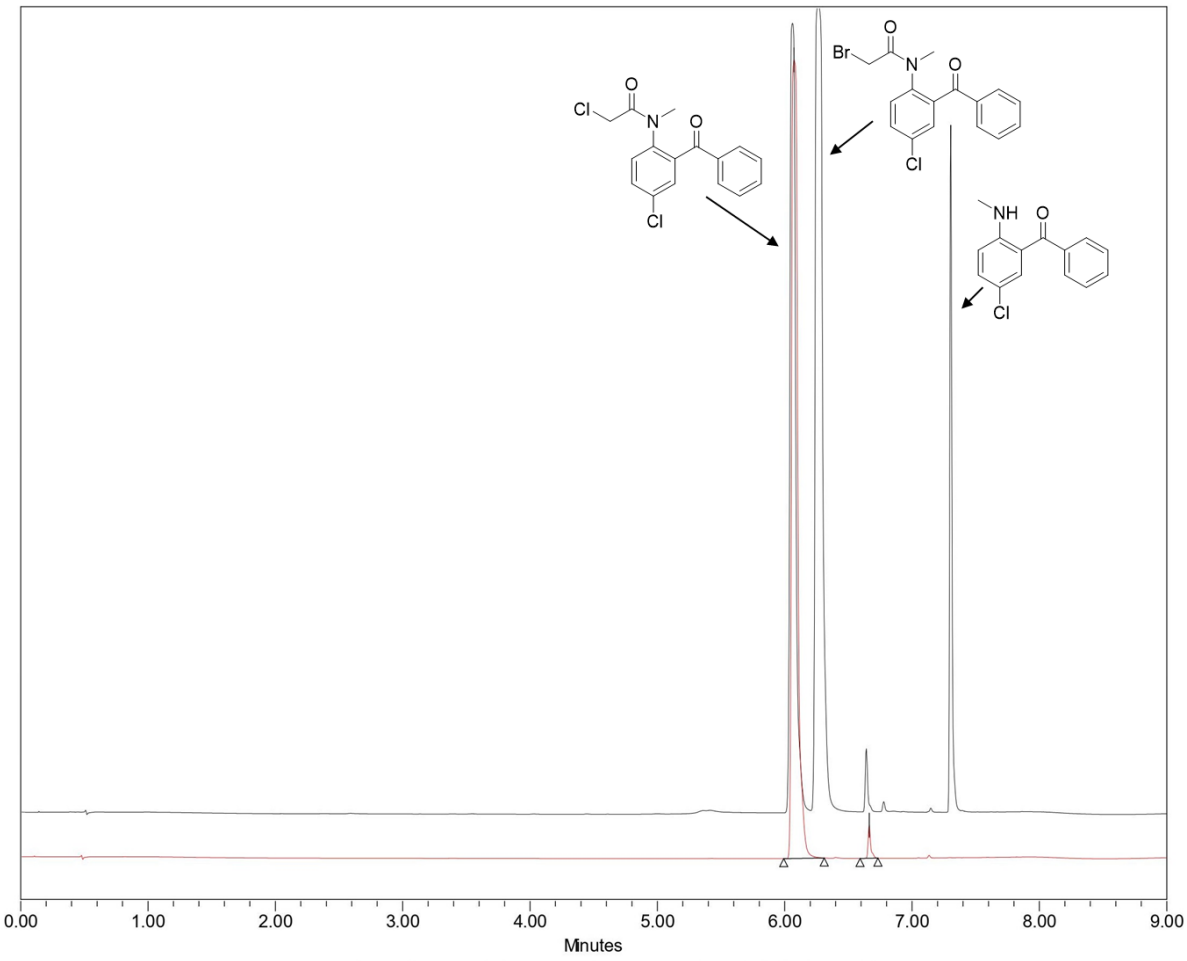

Figure 2.13 UPLC chromatogram of chloride impurity. The product of the above reaction shares the same residence time with the chloride impurity that is prevalent in our batch and flow trials with bromoacetyl chloride. Red line: Product of reaction with chloroacetyl chloride as acylation agent. Black line: Product of reaction with bromoacetyl chloride as acylation agent. Note that both reactions generate a product with a similar retention time (6.1 min).

Chemical tests: To further elucidate whether the impurity is **3b** or **7**, we subjected the product of the above reaction above (red chromatogram) to one of two conditions:

Condition 1: Dissolve 50 mg of impurity in 2 mL NH_3 solution (7N in MeOH) then stir at 80°C overnight. If the impurity is compound **3b**, the conditions will provide diazepam as product.

Condition 2: Dissolve 50 mg of impurity in 2 mL water then stir at 80°C overnight. If the impurity is compound **7**, the conditions will convert the acid chloride into a carboxylic acid.

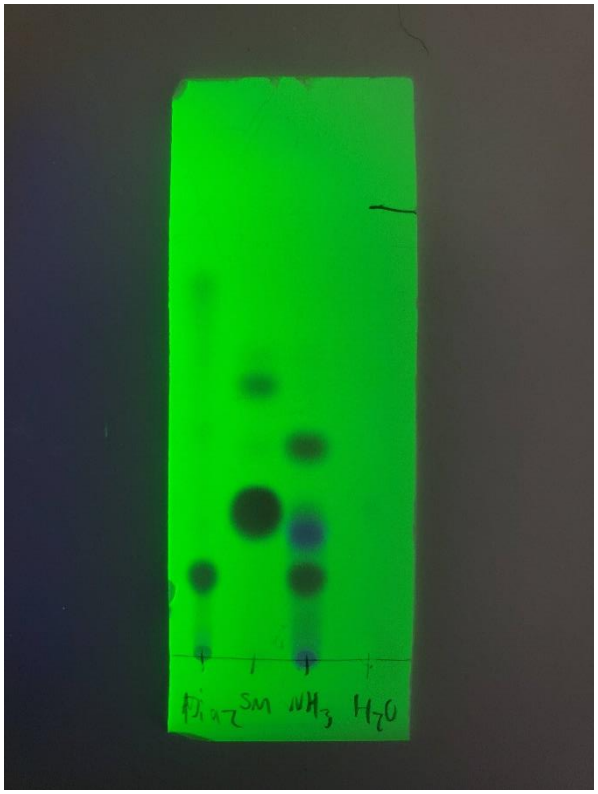

Figure 2.14 TLC of chemically testing chloride impurity. Lanes from left to right: diazepam reference, chloride impurity, product of Condition 1, product of Condition 2. Solvent: 2:1 petroleum ether:ethyl acetate. The lane for Condition 1 has a spot that has a similar retention factor to diazepam. Condition 2 did not seem to product any product as the chloride impurity was insoluble in water. A very faint spot with a retention factor similar to the impurity can be seen in the Condition 2 lane.

Provided the evidence above and the NMR of impurity matching **3a** in the literature, we deduced that chloride impurity **3a** forms in the presence of bromoacetyl chloride as opposed to the S_N2 product that is compound **7**.

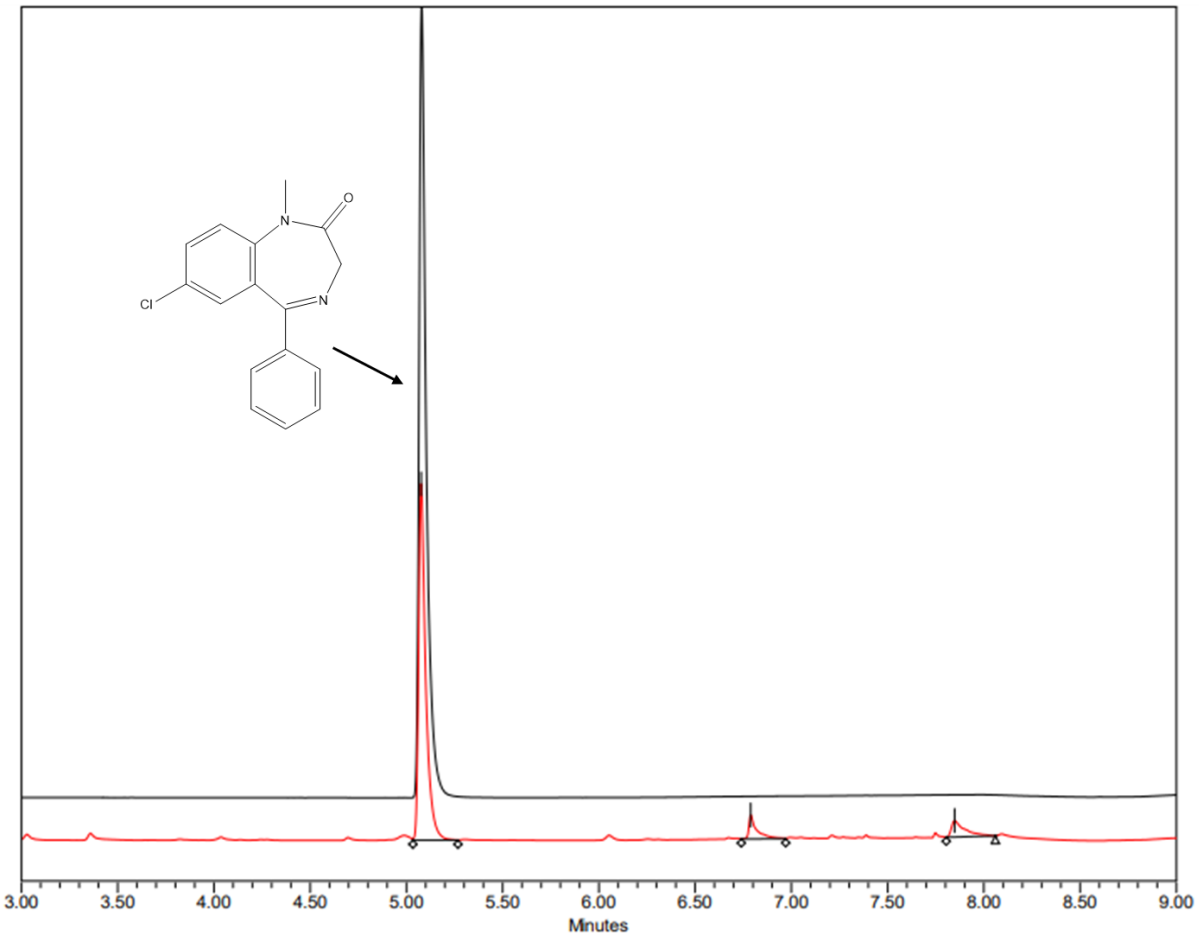

Figure 2.15 Chromatogram of precipitate. A precipitate formed in the reactor channels upon adding NH_4OH/NH_4Br solution. By removing the precipitate and running a UPLC, we observe that this has the same retention time as diazepam. Red line: Isolated precipitate from flow reactor. The prominent peak shares a retention time with diazepam standard (5.1 min). Black line: Diazepam standard.

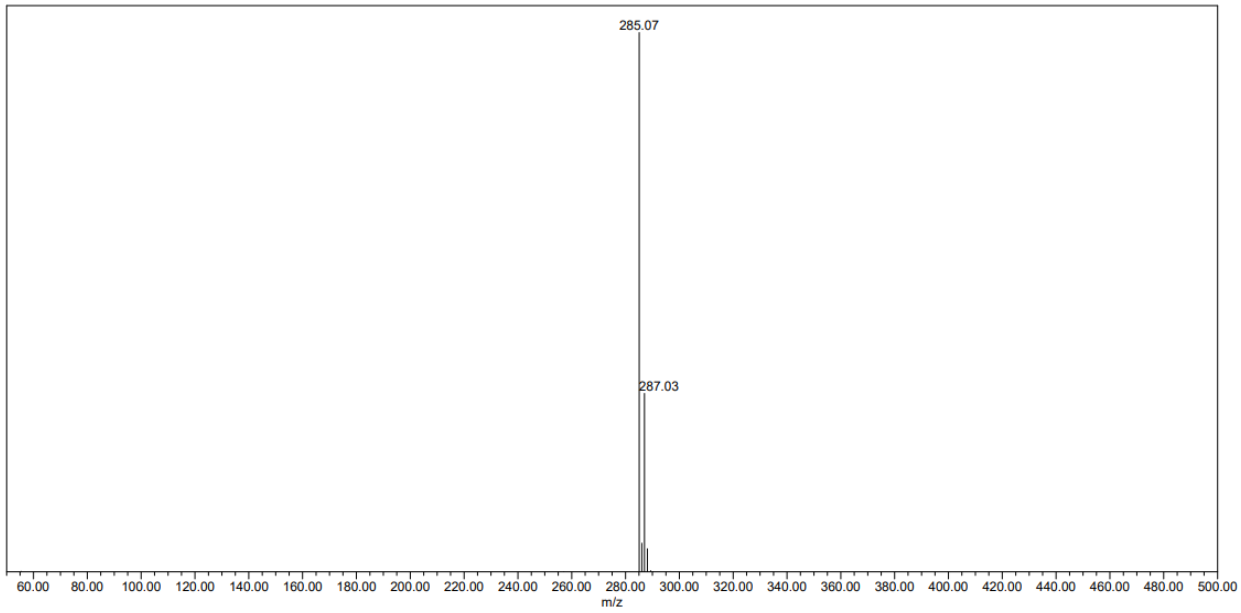

Figure 2.16 Mass spectrum of major UPLC peak from precipitate sample. UPLC-MS was used to obtain the mass of the peak at 5.1 minutes. Base peak matches the $[M+H]^+$ mass of diazepam (MW = 284.7 g/mol).

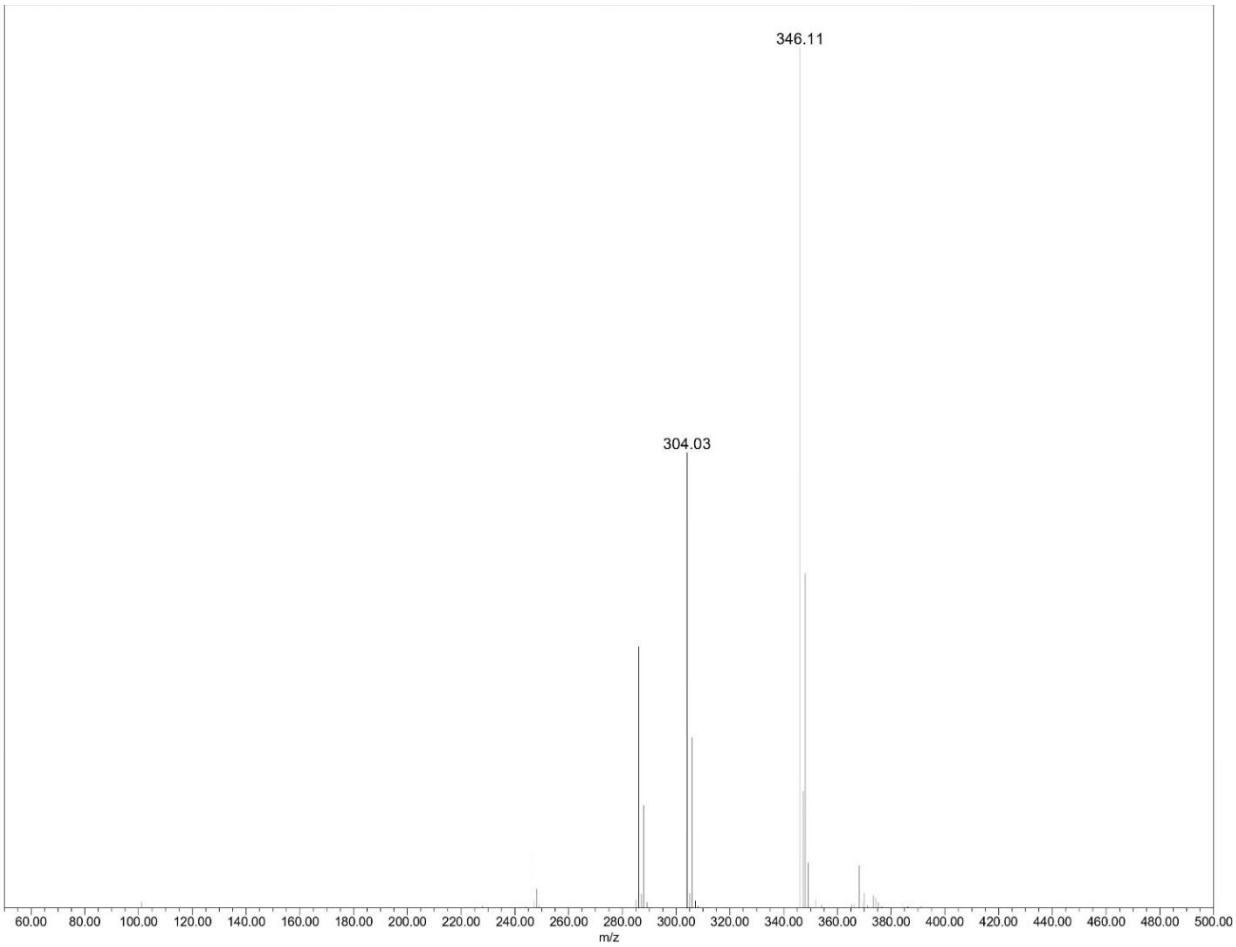

Figure 2.17 Mass spectrum of acetate impurity 6. UPLC-MS was used with a sample from the NH_4OAc trials to obtain the mass of the peak at 5.3 minutes. Base peak matches the $[M+H]^+$ mass of proposed structure **6** (MW = 245.8 g/mol). Fragmentation of acetate provides the m/z peak 304.03.

A)

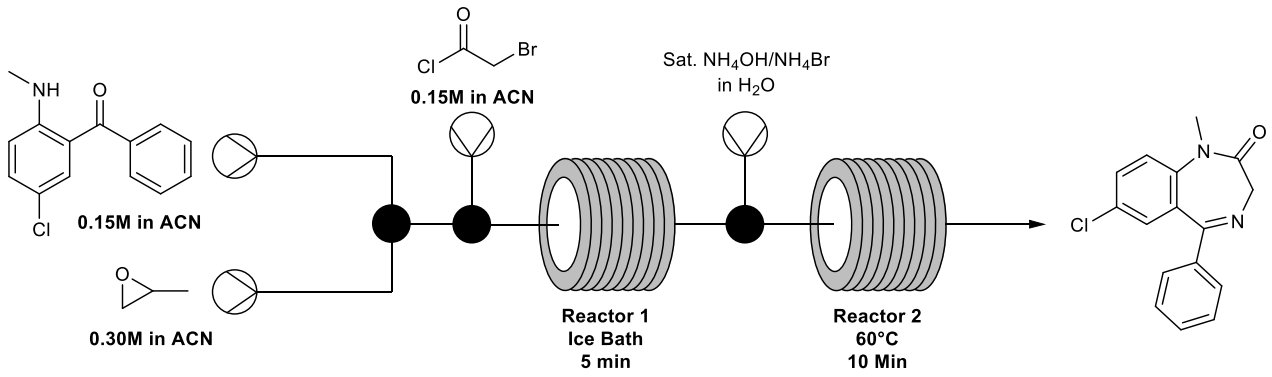

B)

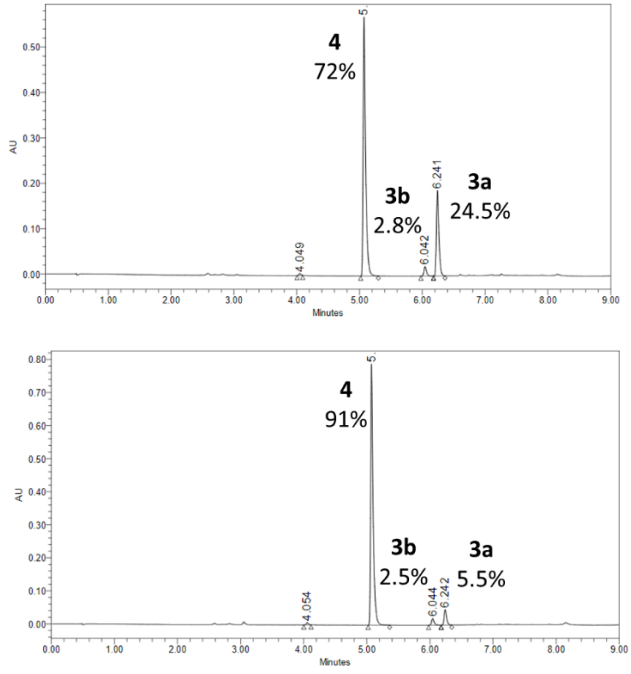

Figure 2.18 Summary of large-scale flow synthesis of diazepam. A) Schematic for large scale synthesis adapted from microscale experiments. Benzophenone, propylene oxide, and acid chloride were loaded into 6 mL gas-tight syringes and pumped at a rate of 10 µL/min. Saturated NH_4OH/NH_4Br solution was loaded into a 10 mL gas-tight syringe and pumped at a rate of 30 µL/min. B) UPLC chromatogram of two 1 hour fractions analyzed prior to purification. Left: Yield = 21.5 mg (84%). Right: Yield = 27.3 mg (106%). Theoretical: 25.6 mg. Yields are based off of theoretical total volume of 3.6 mL that is collected over the course of 1 hour.

Table 2.2 Summary of key batch reactions performed in batch.

Ammonia Source	**Starting Reactant**	**Stages Tested**	**Chemical Conditions**	**Results**
7N NH_3	**3a**	Stage 2	65°C, 1 h, Toluene	**1**: 3%, **4**: 97%; by HPLC
7N NH_3	**3a**	Stage 2	100°C, 1 h, Toluene	**1**: 0.61%, **3a**: 3% **4**: 95%; by HPLC
NH_4OH	**3a**	Stage 2	70°C, 3 h, ACN, Toluene	**1**: 15%, **4**: 65%; by UPLC
NH_4OAc	**1**	Stage 1 and 2 (one-pot)	1) RT, 0.5 h, NMP 2) 60°C, 2 h, H_2O	**4**: 86%; by UPLC
NH_4OAc	**1**	Stage 1 and 2 (one-pot)	1) RT, 0.5 h, NMP 2) 100°C, 1 h, H_2O	**4**: 85%; by UPLC
NH_4OAc	**1**	Stage 1 and 2 (one-pot)	1) RT, 0.5 h, ACN 2) 100°C, 1 h, H_2O	**4**: 87%; by UPLC
NH_4OAc	**3a**	Stage 2	100°C, 1 h, H_2O, ACN, Toluene	TLC collected. SM present after 1 h indicating slowed reaction
NH_4Br/NH_4OH	**3a**	Stage 2	40°C, 2 h, ACN	**3b**: 3%, **4**: 90%; by UPLC
NH_4Br/NH_4OH	**1**	Stage 1 and 2 (one-pot)	1) RT, 0.5 h, ACN 2) 50°C, overnight, water	**3b**: 4%, **4**: 94%; by UPLC

Table 2.3 Optimization of reagent stoichiometries by adjusting flow rates in an automated microfluidic system. Each condition depicts the flow rates of each reagent to achieve the respective equivalents of **2a**. Reagents flowed through reactor chip 3225 (10 µL) with a constant temperature and residence time of 5 minutes.

2a Equivalents	Flow rate **2a** (µL/min)	Flow rate **1** (µL/min)	Flow rate **5** (µL/min)
1.00	0.667	0.667	0.667
1.02	0.675	0.663	0.663
1.04	0.684	0.659	0.659
1.06	0.692	0.654	0.654
1.08	0.700	0.650	0.650
1.10	0.708	0.646	0.646
1.12	0.717	0.642	0.642
1.14	0.725	0.638	0.638
1.16	0.733	0.633	0.633
1.18	0.742	0.629	0.629
1.20	0.750	0.625	0.625

Table 2.4 Results from testing acid chloride equivalence in flow at a 10 minute residence time.

2a Equivalents	% **3a**	% **3b**	% **1**
1.00	86.55	2.29	0
1.02	88.35	2.26	0
1.04	89.01	1.99	0
1.06	89.46	2.27	0
1.08	89.82	2.19	0
1.10	92.81	2.55	0

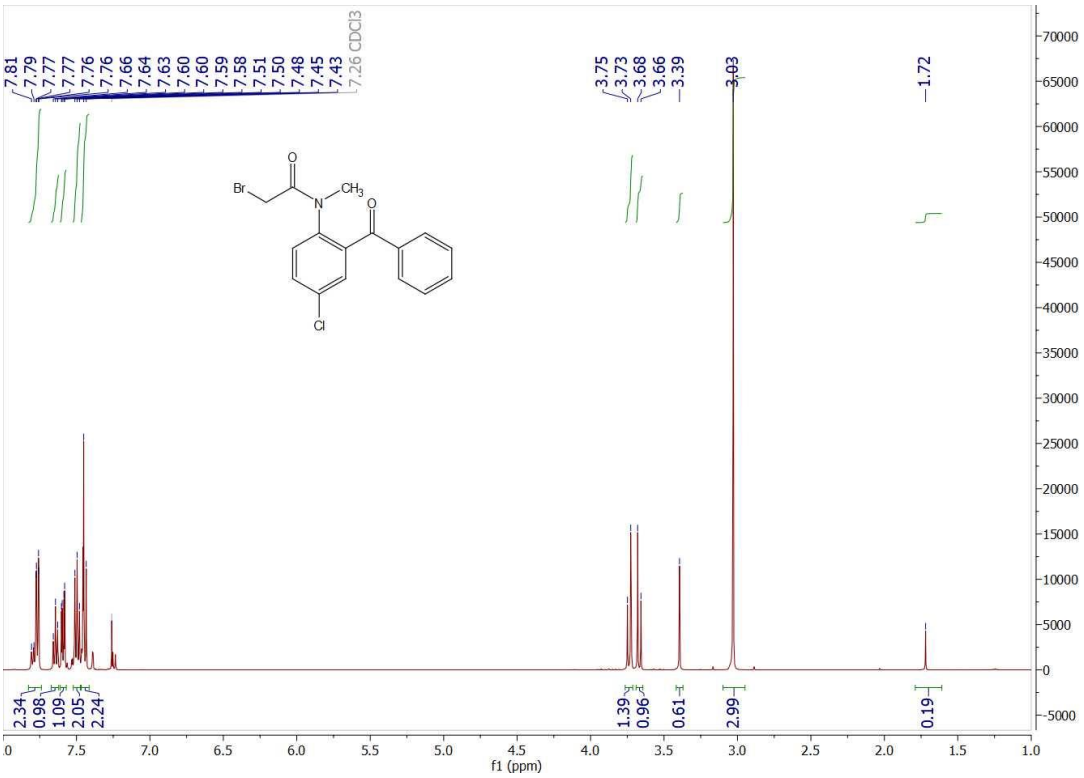

Figure 2.19 ^{1}H NMR of bromide intermediate **3a** dissolved in chloroform.

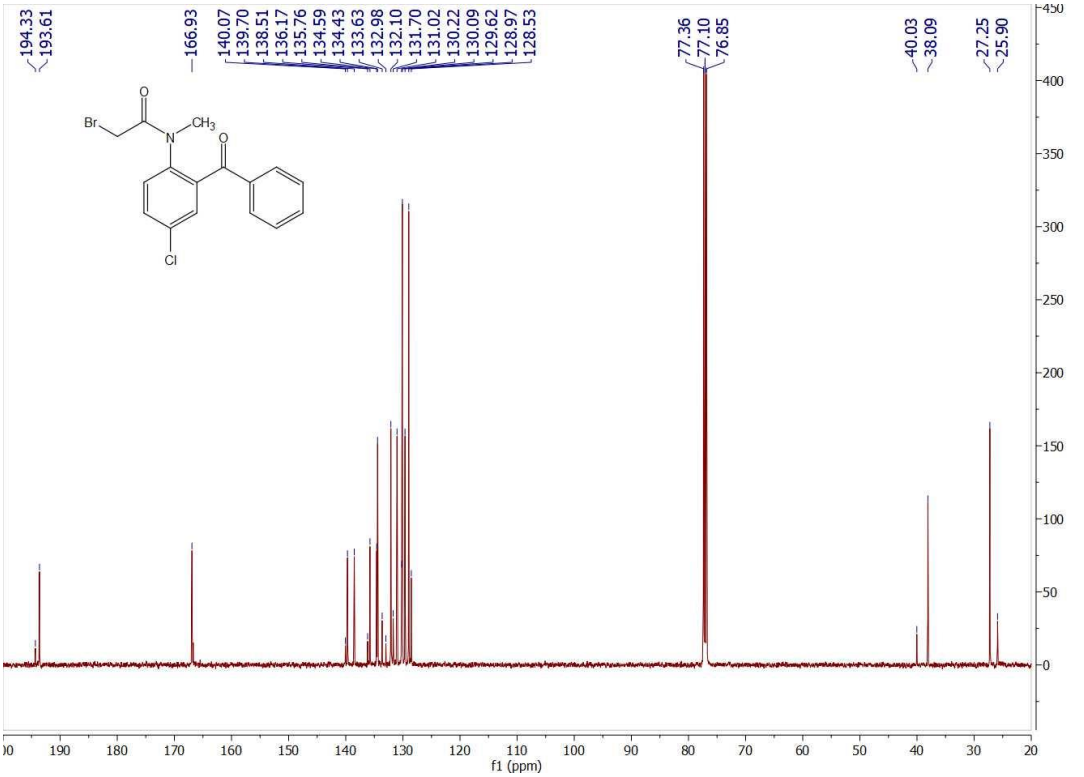

Figure 2.20 ^{13}C NMR of bromide intermediate **3a** dissolved in chloroform.

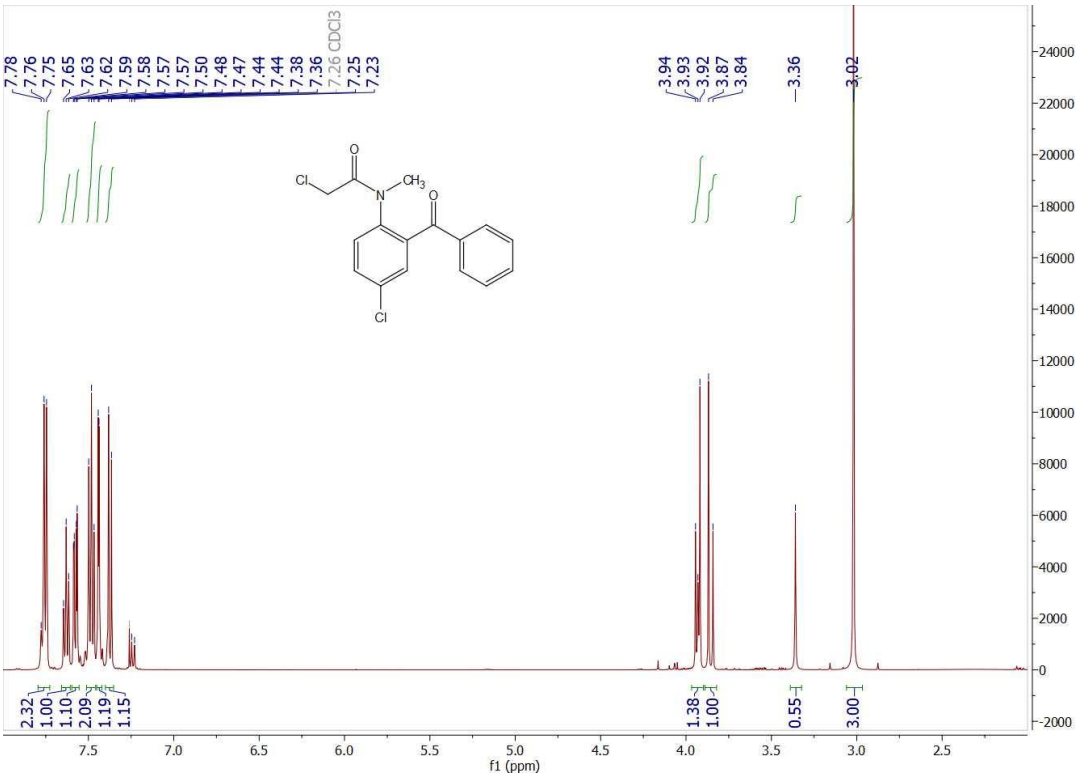

Figure 2.21 ^{1}H NMR of chloride impurity **3b** dissolved in chloroform.

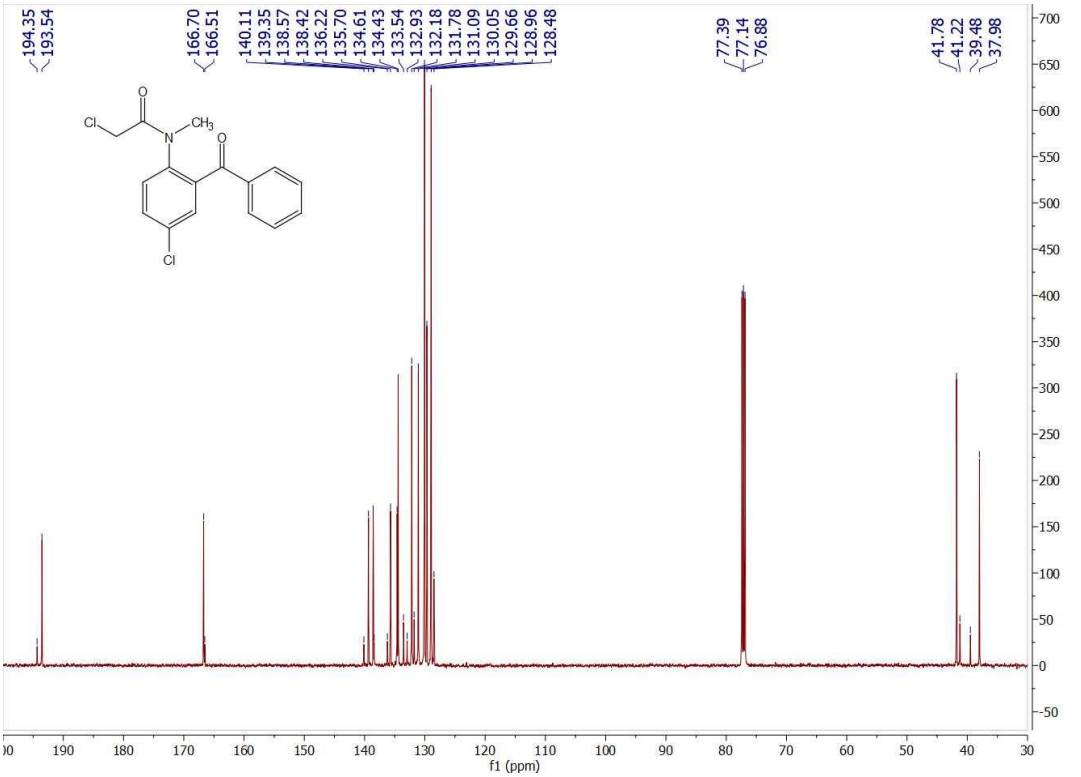

Figure 2.22 ^{13}C NMR of bromide intermediate **3a** dissolved in chloroform.

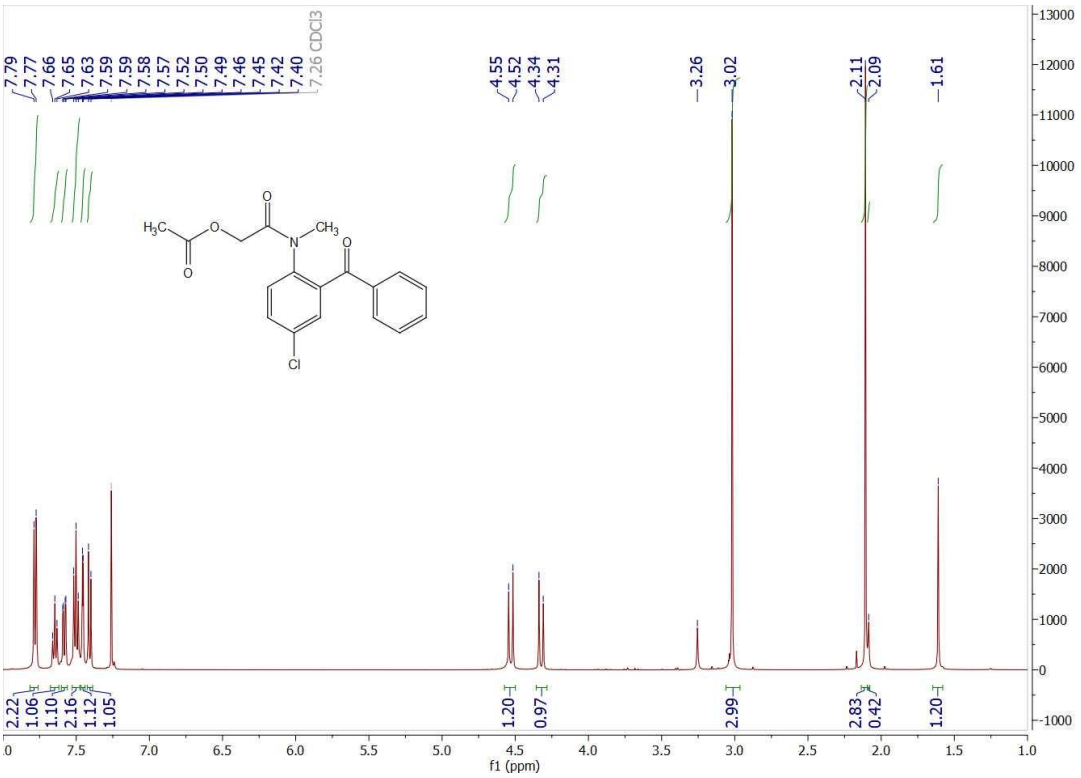

Figure 2.23 ^{1}H NMR of acetate adduct **6** dissolved in chloroform.

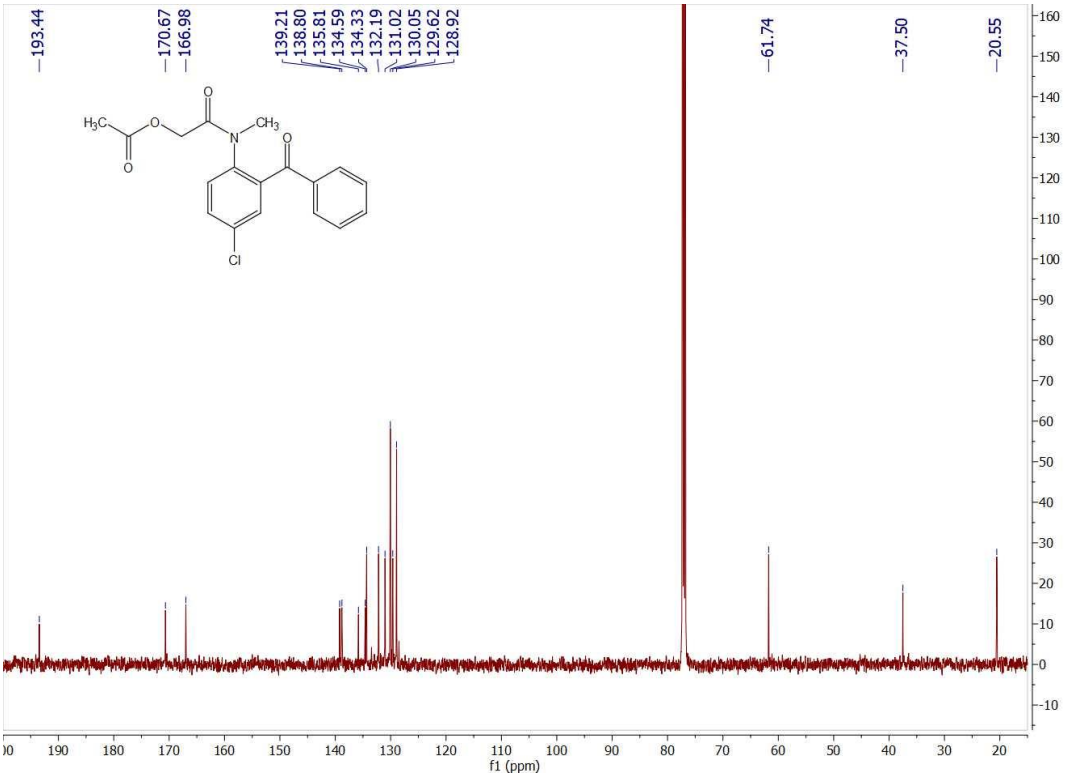

Figure 2.24 ^{13}C NMR of acetate adduct **6** dissolved in chloroform.

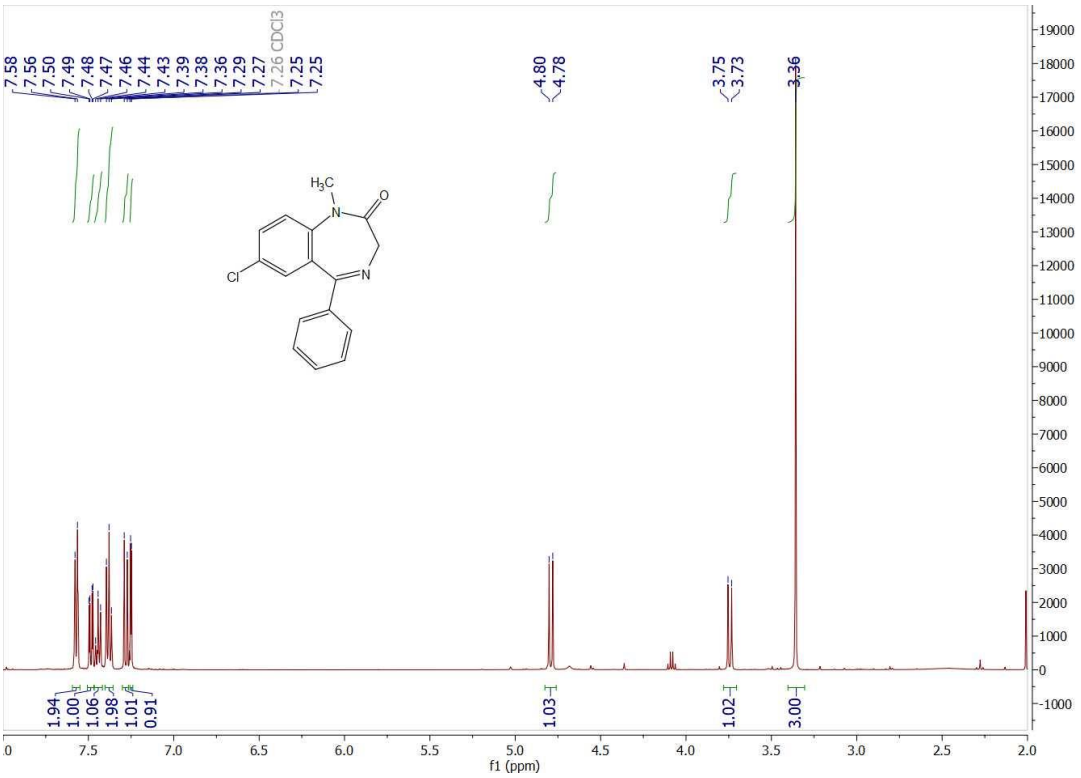

Figure 2.25 ^{1}H NMR of diazepam **4** dissolved in chloroform.

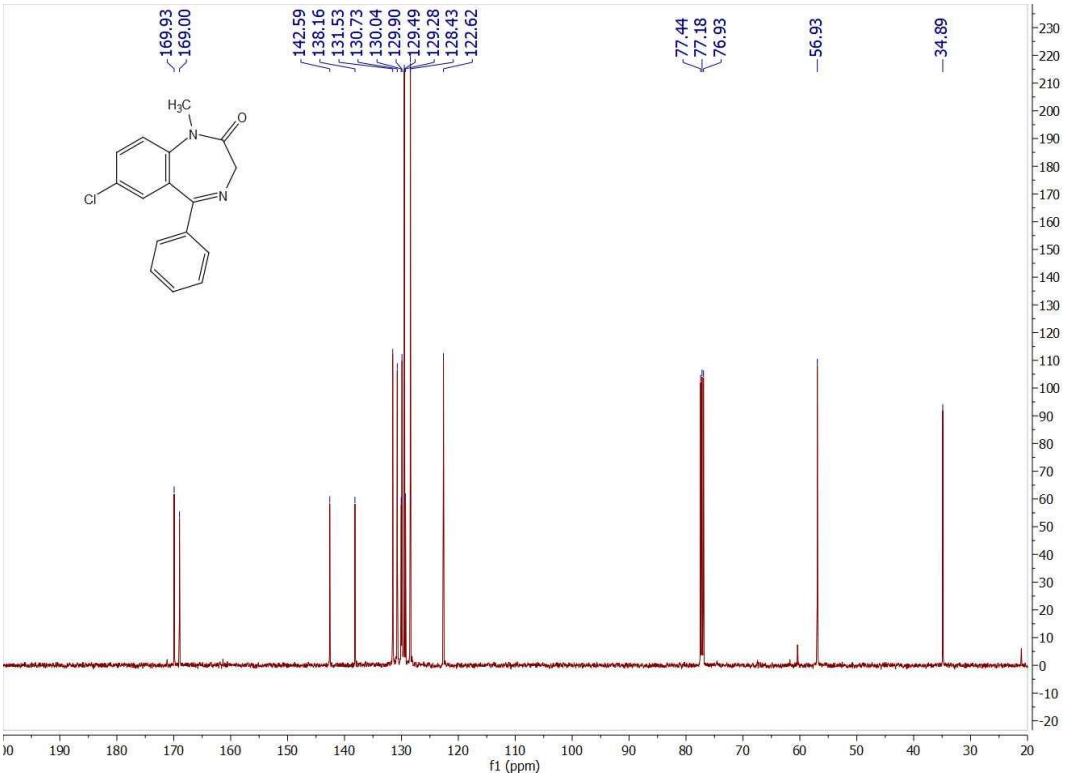

Figure 2.26 ^{13}C NMR of diazepam **4** dissolved in chloroform.

2.6 References

[1] Srai, J. S.; Badman, C.; Krumme, M.; Futran, M.; Johnston, C. Future Supply Chains Enabled by Continuous Processing—Opportunities Challenges May 20–21 2014 Continuous Manufacturing Symposium. *J. Pharm. Sci.* **2015**, *104*, 840–849.

[2] Shukar, S.; Zahoor, F.; Hayat, K.; Saeed, A.; Gillani, A. H.; Omer, S.; Hu, S.; Babar, Z.-U.-D.; Fang, Y.; Yang, C. Drug Shortage: Causes, Impact, and Mitigation Strategies. *Front. Pharmacol.* **2021**, *12*, 693426.

[3] Burcham, C. L.; Florence, A. J.; Johnson, M. D. Continuous Manufacturing in Pharmaceutical Process Development and Manufacturing. *Annu. Rev. Chem. Biomol. Eng.* **2018**, *9* (1), 253–281.

[4] Ali, M. S.; Hooshmand, N.; El-Sayed, M.; Labouta, H. I. Microfluidics for Development of Lipid Nanoparticles: Paving the Way for Nucleic Acids to the Clinic. *ACS Appl. Bio Mater.* **2021**.

[5] Chen, Y.; Glotz, G.; Cantillo, D.; Kappe, C. O. Organophotocatalytic N-Demethylation of Oxycodone Using Molecular Oxygen. *Chem. – Eur. J.* **2020**, *26* (13), 2973–2979.

[6] Jaman, Z.; Sobreira, T. J. P.; Mufti, A.; Ferreira, C. R.; Cooks, R. G.; Thompson, D. H. Rapid On-Demand Synthesis of Lomustine under Continuous Flow Conditions. *Org. Process Res. Dev.* **2019**, *23* (3), 334–341.

[7] Ziegler, R. E.; Desai, B. K.; Jee, J.-A.; Gupton, B. F.; Roper, T. D.; Jamison, T. F. 7-Step Flow Synthesis of the HIV Integrase Inhibitor Dolutegravir. *Angew. Chem.* **2018**, *130* (24), 7299–7303.

[8] Hopkin, M. D.; Baxendale, I. R.; Ley, S. V. A Flow-Based Synthesis of Imatinib: The API of Gleevec. *Chem. Commun.* **2010**, *46* (14), 2450–2452.

[9] Cole, K. P.; Groh, J. M.; Johnson, M. D.; Burcham, C. L.; Campbell, B. M.; et al. Kilogram-Scale Prexasertib Monolactate Monohydrate Synthesis under Continuous-Flow CGMP Conditions. *Science* **2017**, *356* (6343), 1144–1150.

[10] World Health Organization. *Model. Lists of Essential Medicines 2019*; World Health Organization: Geneva, Switzerland, 2019.

[11] Fuentes, A. V.; Pineda, M. D.; Venkata, K. C. N. Comprehension of Top 200 Prescribed Drugs in the US as a Resource for Pharmacy Teaching, Training and Practice. *Pharmacy* **2018**, *6* (2), 43.

[12] Shtull-Leber, E.; Silbergleit, R.; Meurer, W. J. Pre-Hospital Midazolam for Benzodiazepine-Treated Seizures before and after the Rapid Anticonvulsant Medication Prior to Arrival Trial: A National Observational Cohort Study. *PLOS ONE* **2017**, *12* (3), e0173539.

[13] Bachhuber, M. A.; Hennessy, S.; Cunningham, C. O.; Starrels, J. L. Increasing Benzodiazepine Prescriptions and Overdose Mortality in the United States, 1996–2013. *Am. J. Public Health* **2016**, *106* (4), 686.

[14] Agarwal, S. D.; Landon, B. E. Patterns in Outpatient Benzodiazepine Prescribing in the United States. *JAMA Netw. Open* **2019**, *2* (1), e187399.

[15] Ewan, H. S.; Iyer, K.; Hyun, S.-H.; Wleklinski, M.; Cooks, R. G.; Thompson, D. H. Multistep Flow Synthesis of Diazepam Guided by Droplet-Accelerated Reaction Screening with Mechanistic Insights from Rapid Mass Spectrometry Analysis. *Org. Process Res. Dev.* **2017**, *21* (10), 1566–1570.

[16] Adamo, A.; Beingessner, R. L.; Behnam, M.; Chen, J.; Jamison, T. F.; et al. On-Demand Continuous-Flow Production of Pharmaceuticals in a Compact, Reconfigurable System. *Science* **2016**, *352* (6281), 61–67.

[17] Rogers, L.; Briggs, N.; Achermann, R.; Adamo, A.; Azad, M.; et al. Continuous Production of Five Active Pharmaceutical Ingredients in Flexible Plug-and-Play Modules: A Demonstration Campaign. *Org. Process Res. Dev.* **2020**, *24* (10), 2183–2196.

[18] Collins, N.; Stout, D.; Lim, J.-P.; Malerich, J. P.; White, J. D.; et al. Fully Automated Chemical Synthesis: Toward the Universal Synthesizer. *Org. Process Res. Dev.* **2020**, *24* (10), 2064–2077.

[19] Bédard, A.-C.; Longstreet, A. R.; Britton, J.; Wang, Y.; Moriguchi, H.; et al. Minimizing E-Factor in the Continuous-Flow Synthesis of Diazepam and Atropine. *Bioorg. Med. Chem.* **2017**, *25* (23), 6233–6241.

[20] Feng, Y.; Xie, R.; Wu, Z.; Marsh, K. N. Vapor−Liquid Equilibria for Ammonia + Methanol. J. Chem. Eng. Data 1999, 44 (3), 401–404.

[21] Balaji, B. S.; Dalal, N. An Expedient and Rapid Green Chemical Synthesis of N-Chloroacetanilides and Amides Using Acid Chlorides under Metal-Free Neutral Conditions. *Green Chem. Lett. Rev.* **2018**, *11* (4), 552–558.

[22] Phillips, R. E.; Soulen, R. L. Propylene Oxide Addition to Hydrochloric Acid: A Textbook Error. *J. Chem. Educ.* **1995**, *72* (7), 624.

[23] Dhaon, M. K. Use of Propylene Oxide as an Acid Scavenger in Peptide Synthesis. US5698676A, December 16, 1997.